nature portfolio

Peer Review File

# TGFβ-mediated dural progenitor cell migration into the coronal suture is crucial for preventing craniosynostosis

Corresponding Author: Dr Yang Chai

**This file contains all reviewer reports in order by version, followed by all author rebuttals in order by version.**

Version 0:

Reviewer comments:

Reviewer #1

(Remarks to the Author)
The study proposes an intriguing theory that neural crest-derived dural cells migrate specifically into the coronal suture during postnatal development in a manner directed by suture-to-dura TGFb signaling, which may explain the preferential involvement of the coronal suture in syndromic craniosynostosis. The authors supported this theory by leveraging Gli1-Cre-based lineage tracing and Tgfbr2 conditional deletion coupled with allograft suture transplantation experiments. The authors further identified decorin as a potential TGFb inhibitor, the inhibition of which rescues Twist1 heterozygosity-induced coronal suture synostosis. Overall, the study highlights a novel mechanism of coronal suture formation and explains its susceptibility to craniosynostosis. It also challenges the prevailing concept that undifferentiated cells in the middle of the suture are the source of other mesenchymal cells. The biological significance of the study is high. The authors should strengthen the study's rigor by addressing the following points.

1. To confirm the reproducibility of the findings, the authors should clarify the number of animals (biological replicates) in each experiment while providing the quantification of the key results, as appropriate. In many instances, the data lack the sample size description and quantification, making it difficult to judge if the presented results are reproducible. The individual points are described below.

2. The study's key assumption is that suture-to-dura TGFb receptor signaling specifically occurs in the coronal suture. To further support this premise, the authors should expand Figure 2-h and define the expression patterns of TGFB1-3 and Tgfrb2 in other neural crest and mesoderm-derived sutures, such as sagittal and lambdoid sutures. This information is needed to strengthen the study's significance.

3. The suture allograft in Figure 4 provides vital evidence for dural cells not migrating into the suture without TGFb signaling, resulting in suture fusion. However, additional controls are needed to support this conclusion fully. First, the authors need to transplant other WT sutures (sagittal or lamboid) into the control and mutant recipients. If the authors' hypothesis is correct, tdT+ cells should not migrate into the suture even in the control recipient. Also, the authors should transplant the donor suture into other sutures (either sagittal or lamboid) of the recipient mice. These additional experiments will provide more solid evidence for the specific requirement of TGFb signaling in the coronal suture in an allograft setting.

4. The authors should also investigate the potential role of dura-to-suture signals in premature coronal suture fusion. Supplementary Figure 5 shows that the loss of cell proliferation and progenitors occurs acutely upon the loss of Tgfrb2 in Gli1+ cells, long before cell migration occurs, strongly indicating that non-cell-autonomous mechanisms are involved. Mechanisms of premature suture fusion cannot be entirely attributed to defective cell migration. What are the candidates of this dura-to-suture signal? The authors should delve into the RNA-seq datasets, identify potential signaling pathways, and validate the expression patterns using IHC/ISH.

5. The manuscript lacks the details regarding ex vivo calvarial organ culture, which provides key evidence that dural cells migrate into the coronal suture. How were sutures and dura separated, stained separately, and recombined? There is a technical concern that Q-tracker dyes diffuse the tissue boundaries and stain suture cells without cell migration. The authors should confirm the validity of this approach by genetic marking, using a nuclear fluorescent reporter that does not diffuse across tissue.

6. How does decorin inhibit TGFb in the coronal suture? Does decorin sequester TGFb in the ECM, or does it bind to the receptor? The authors should examine if decorin directly binds to TGFb in the suture by immunohistochemical approaches, such as colocalization.

7. A dura-specific marker (such as Rbp1/RBP1) should be used to demonstrate the localization of some important readouts, such as Q-tracker, Tgfrb2, and Gli1-tdT. The individual points are described below.

Individual points:

8. Abstract
- Line 33: The authors should clarify that decorin is upregulated in Twist mutant mice, which leads to dampened TGFb signaling.
- Line 34: The authors did not really show the data that “restoring TGFb signaling rescues coronal suture patency in Twist+/- mice”. It is only decorin inhibition by shRNA that rescued the phenotype. The authors should be explicit about this.
- Line 36: As mentioned above, it is not only dural cell migration that contributes to coronal fusion. A dura-to-suture signal appears to be involved as well. The authors should remain open to this possibility.

9. Introduction
- Lines 70-73: The authors should mention decorin upregulation as a mechanism for impaired TGFb signaling.

10. Results
- Lines 85-86: Figure 1b. The authors should use a dura-specific marker to highlight the structure. The distinction between the frontal bone and the dura mater is obscure.
- Lines 89-91: Figure 1c-f. The authors quantify the number of tdT+ cells in the suture mesenchyme across biological replicates and provide a graph.
- Lines 98-99: The authors should explain in detail in the main text how the ex vivo organ culture model was performed, and how a dye stained the underlying dura. A dura-specific marker should also confirm the validity of dye staining.
- Line 111-112: According to Figure 1d, it is not only the frontal bone cells that were genetically labeled by ZsGreen. Some of the suture mesenchymal cells are also marked. The authors should clarify.
- Line 175-176: Figure 3e-j. The authors should clarify how many biologically independent animals they examined and describe the penetrance of the phenotype. Did all the mutant mice show craniosynostosis specifically in the coronal suture? Did the authors look at both male and female mice?
- Lines 213-216: The authors should clarify if these results were observed across biological replicates.
- Lines 220-221: Figure 5d-f. The concern is that Q-tracker can diffuse across tissues, as there are some signals in the frontal and parietal bones.
- Lines 283-284: Figure 7d-f. The authors should also inject decorin protein in other sutures (sagittal or lamboid) to examine if it causes partial suture fusion.

11. Materials and Methods
- Lines 758-768: This section on developing mouse brain volume calculation is irrelevant to the current manuscript.

12. Figures
- Figure 1g-h: The Q-tracker signal in the suture after organ culture should be quantified across biological replicates.
- Figure 1j-o: The ZsGreen and tdT signals in the suture after allograft should be quantified across biological replicates.
- Figure 3a-d: The quantification of Tgfbr2 and p-SMAD2 signal is needed.
- Figure 4d-i: The authors should clarify if these results were observed across biological replicates and provide quantification, as appropriate.

Reviewer #2

(Remarks to the Author)
Chen et al. Present a tour de force of developmental biology and genetics that is impressive in its breadth of techniques and convincing mechanistic insights. The authors explore why the coronal suture, as oppose to the other sutures of the skull vault, are differently affected in disease. Although during embryonic stages, the coronal suture is mesoderm-derived, the authors use a genetic reporter to find increasing numbers of neural crest cells in the coronal sutures during postnatal development. The authors find neural crest cells invade the suture from the underlying dural cells specifically in the coronal suture, using in and ex vivo lineage tracing. This invasion is attributed to increased proliferation of DuSCs which then migrate into the coronal suture. Analysis of various sequencing data sets implicated TGFbeta signaling in promoting dural cell invasion. The authors confirmed this link through genetic and chemical abrogation of TGFβ which caused coronal synostosis and reduced dural-derived stem cell invasion. These data were consistent with the reduced TGFβ signaling found in Twist1 mutants which develop coronal synostosis. An inhibitor of TGFβ, Decorin (Dcn), was increased in mutant coronal sutures raising the hypothesis that Dcn limits migration of DuSCs into the suture mesenchyme by modulating TGFβ signaling between suture mesenchyme and the dura. Coronal synostosis and loss of DuSC invasion into the suture was found in Dcn treated animals, confirming a role for Suture-Dura TGFβ signaling in directing DuSCs into the coronal suture mesenchyme. These data provide a beautiful cell biological understanding of suture biology that has significant implications for treating human disease.

The manuscript presented by Chen et al. is of very high quality and provides exciting and important intellectual and technical

advancements in craniofacial biology and development more broadly. This reviewer is extremely excited by this manuscript and looks forward to its publication, although very minor points should be addressed.

1. Ref 20 doesn't seem appropriate as this is not original Mesp1 data and does not show data or illustrations pertaining to the skull. Other publications better show the Mesp1 label at the coronal suture (e.g. Yen et al. 2010, Tabler et al. 2016, Larsen's Human Embryology etc).

2. Ref 18 refers to labelling of dissociated suture cells with Q Tracker performed in previous work from the Chai lab. However, that protocol is quite different from the experiment described here where only exposed cells of the explant take up the Q tracker nanocrystals. It would help to describe the experiment more thoroughly in this manuscript (even if just in the methods) as some may be concerned that the dye is easily incorporated into cells other than the dura. However, the large 2um size of the nanocrystals makes it unlikely that QTracker nanodots will be taken up accept by cells directly exposed to dye-containing media. This should be explicitly stated for others to understand and help strengthen the claim that only dural cells are labelled in explant experiments.

3. (i) Line 135: 'DuSC migratory capacity and EdU incorporation (Supplementary Fig. 2b-g), indicating enhanced migration and proliferation compared to controls…SuSCs can enhance DuSC migration and proliferation.'- While a common assumption in scratch assays, the inference of cell migration is not strictly correct without additional experiments. The increase in proliferation found when incubating DuSCs or SuSCs in suture conditioned media could be sufficient to explain the wound healing assays without requiring migration (see Ranft et al. 2010: Mechanically driven interface propagation in biological tissues, and Cochet-Escartin and Ranft et al. 2014: Border Forces and Friction Control Epithelial Closure Dynamics, or indeed ref 20 Dahmann et al. 2011). The increase in proliferation is nonetheless good evidence of stem cell behavior where division is an important part of stem cell mobilization in repair. To be confident that cell migration is increased in these assays, cell tracking, a measure of cell mixing, or cell density vs scratch closure could be assayed. As much of the field fails to recognize these limitations of scratch assays and authors continue to uphold them as tests of migration, it is not essential to change these statements in the manuscript. However, without toning down or specifying the limitations of these assays, the quality of the work is undermined and, in this case, may impact the long-Gevity of the work.

3. (ii) A similar problem arises in Results for Figure 6, Line 281: 'This treatment suppressed the migration-promoting effect of SuSC-CM (Fig. 6r-s), indicating that Decorin inhibits dural cell migration.'. In the absence of cell tracking, it is not technically true that these data demonstrate Dcn as a regulator of dural cell migration. As there is no metric of cell proliferation for these samples, it is also not clear whether Dcn treatment phenocopies the Tgfβ deletion. Comparing cell density between start and end of scratch assay could be sufficient to extract an effective proliferation metric. The claim that Dcn inhibits migration would therefore be more convincing If proliferation is not increased or density is far lower despite increased proliferation.

4. Sup fig. 2: Quantification of EdU experiments should accompany the image panels, in particular, because the cell densities appear quite different between each condition.

5. Sup Fig. 5: Although consistent with data throughout the paper, Sup Fig 5 does not demonstrate a reduced progenitor pool in animals with Tgfbr2 mutant Gli1 cells, although it does show their proliferation is reduced. Testing this claim definitively would require a metric of suture mesenchyme cell density/width or quantifying Maff, Lepr, or ccl7 expressing cells in situ or through sequencing. Toning down the title of this figure would be sufficient to address this concern.

6. Is it known whether any mesodermal mesenchyme expresses Wnt1 postnatally? Is it possible that these cells are coming from later Wnt1 expressing cells that are not neural crest? Not essential to address but may be a concern for some and can potentially be extracted from scRNA sequencing data or other published work.

7. Sections of mice treated with Decorin presented in Figure 7e-f appear as though bone fusion is most pronounced on the dural side of the suture. Is this consistent across samples? If so, mentioning this in the results or discussion could further bolster the claim that DuSCs replenish the suture stem cell niche as the dural aspect of the suture would be most affected if the Author's hypothesis is correct. One way to express this would be to measure the width of the suture at the tips of FB and PB and through the centre of the suture. It is not necessary to add these data but these would further support the authors claims.

Version 1:

Reviewer comments:

Reviewer #1

(Remarks to the Author)
The authors have addressed my queries in depth through additional experiments. Specifically, the expansion of the allograft suture transplantation experiments, as detailed in the revised Figure 2, has significantly strengthened the rigor of the current findings.

1. Regarding my previous second point, the authors provided evidence that Tgfrb2 is selectively expressed in the dura below the coronal suture (Fig.3h), unlike in other sutures where Tgfrb2 expression is more widespread (Supplementary Fig. 7j,l,n). The description of these results in the revised main text (Lines 254-265) should be improved. To better contextualize

these findings, the authors should emphasize that Tgfrb2 is most prominently expressed in the dura of the coronal suture, but not in that of other sutures. This claim can also be supported quantitatively by quantifying the ISH signal in the dura across four different sutures.

2. The switch from Q-tracker organ culture to DiI transplantation is reasonable, enhancing the rigor of the study. However, to demonstrate the validity of this approach, the authors would need an additional control to definitively show that the dura DiI signal expansion into the suture mesenchyme after transplantation is not due to passive diffusion. A critical control would be sagittal suture transplantation onto a DiI-labelled dura (of the sagittal suture), which should not show any dura DiI signal in the suture mesenchyme after transplantation, if the authors' premise is correct.

3. Some of the important information added in response to the reviewer's comments is exclusively available as reviewer-only figures, with no description or data added to the main text. The findings regarding other potential signals mediating dure-to-suture interactions (Response letter Fig.1), demonstration of suture transplantation surgery procedure (Response letter Fig.2), co-localization of TGFb ligands and decorin in coronal sutures (Response letter Fig.3), and the specificity of tdT to the dura (Rbp1) are all essential for interpreting the results of the current manuscript. They should be included in Supplementary Figures and mentioned in the main text.

Reviewer #2

(Remarks to the Author)
Chen et al. present an impressive revision of their previous submission which suggested dural cell migration mediated by Tgfbeta pathway activity is uniquely required for coronal suture patency. Their previous ex vivo culture experiments have been replaced by far more convincing in vivo grafting experiments that recapitulate previous findings and add significantly to the narrative. Taken together, the additional experiments strongly support the author's assertion that disrupted Tgfbeta activity, modulated by extracellular decorin, contributes to the pathophysiology of Saethre-Chotzen syndrome and explains differences in suture fusion across the skull cap.

The author's heroic efforts to confirm their hypothesis in vivo are important additions to this manuscript. These are convincing experiments with broad implications for disease and skull development generally. The references to cell mobilisation are well constructed and satisfy intellectual concerns in the prior drafts while also enriching the conclusions of the work. Overall, this reviewer is satisfied with the changes to the submitted work and am excited by the findings!

**REVIEWER COMMENTS**

**Reviewer #1 (Remarks to the Author):**

**The study proposes an intriguing theory that neural crest-derived dural cells migrate specifically into the coronal suture during postnatal development in a manner directed by suture-to-dura TGFb signaling, which may explain the preferential involvement of the coronal suture in syndromic craniosynostosis. The authors supported this theory by leveraging Gli1-Cre-based lineage tracing and Tgfbr2 conditional deletion coupled with allograft suture transplantation experiments. The authors further identified decorin as a potential TGFb inhibitor, the inhibition of which rescues Twist1 heterozygosity-induced coronal suture synostosis. Overall, the study highlights a novel mechanism of coronal suture formation and explains its susceptibility to craniosynostosis. It also challenges the prevailing concept that undifferentiated cells in the middle of the suture are the source of other mesenchymal cells. The biological significance of the study is high. The authors should strengthen the study's rigor by addressing the following points.**

We appreciate the reviewer's comments on our findings and have provided additional data in the revised manuscript to address all the reviewer's questions. Please see our point-by-point responses below.

**1. To confirm the reproducibility of the findings, the authors should clarify the number of animals (biological replicates) in each experiment while providing the quantification of the key results, as appropriate. In many instances, the data lack the sample size description and quantification, making it difficult to judge if the presented results are reproducible. The individual points are described below.**

We thank the reviewer for this suggestion. We have now added the number of biological replicates to each experiment and figure legend. At least 3 individual biological samples were used for each experiment. In addition, quantification with an exact p-value has been provided for all key results, allowing the reproducibility of the findings to be clearly assessed.

**2. The study's key assumption is that suture-to-dura TGFb receptor signaling specifically occurs in the coronal suture. To further support this premise, the authors should expand Figure 2-h and define the expression patterns of TGFB1-3 and Tgfrb2 in other neural crest and mesoderm-derived sutures, such as sagittal and lambdoid sutures. This information is needed to strengthen the study's significance.**

We thank the reviewer for this insightful suggestion. We have included additional results for TGFβ1-3 and *Tgfbr2* in other cranial sutures, including the sagittal, frontal, and lambdoid sutures (**Supplementary Fig. 7i-n and lines 251 to 267**), to further support the importance of suture-to-dura TGFβ signaling during postnatal coronal suture development. In the frontal suture, TGFβ1-3 exhibited expression along the osteogenic fronts of the frontal bones and within the suture mesenchyme, with enrichment near the periosteal surface. *Tgfbr2* expression was broadly distributed in both the suture mesenchyme and frontal bone, indicating widespread responsiveness to TGFβ ligands. In the sagittal suture, all three TGFβ ligands were detected along the periosteum and within the dura mater region. *Tgfbr2* is expressed throughout the suture mesenchyme and dura mater, indicating that TGFβ signaling could originate from the dura and be received by the dura or suture mesenchyme. In the lambdoid suture, TGFβ1-3 showed robust expression in the periosteum and dura mater, as well as within the suture mesenchyme. *Tgfbr2* was mainly expressed across the suture mesenchyme, indicating that TGFβ could be from dura to suture mesenchyme. However, *Tgfbr2* expression was more restricted to the dura in the coronal suture compared to the lambdoid, sagittal, and frontal sutures, suggesting this signaling is more likely to be involved in regulating interaction between suture mesenchyme and dura during postnatal coronal suture development and patency maintenance.

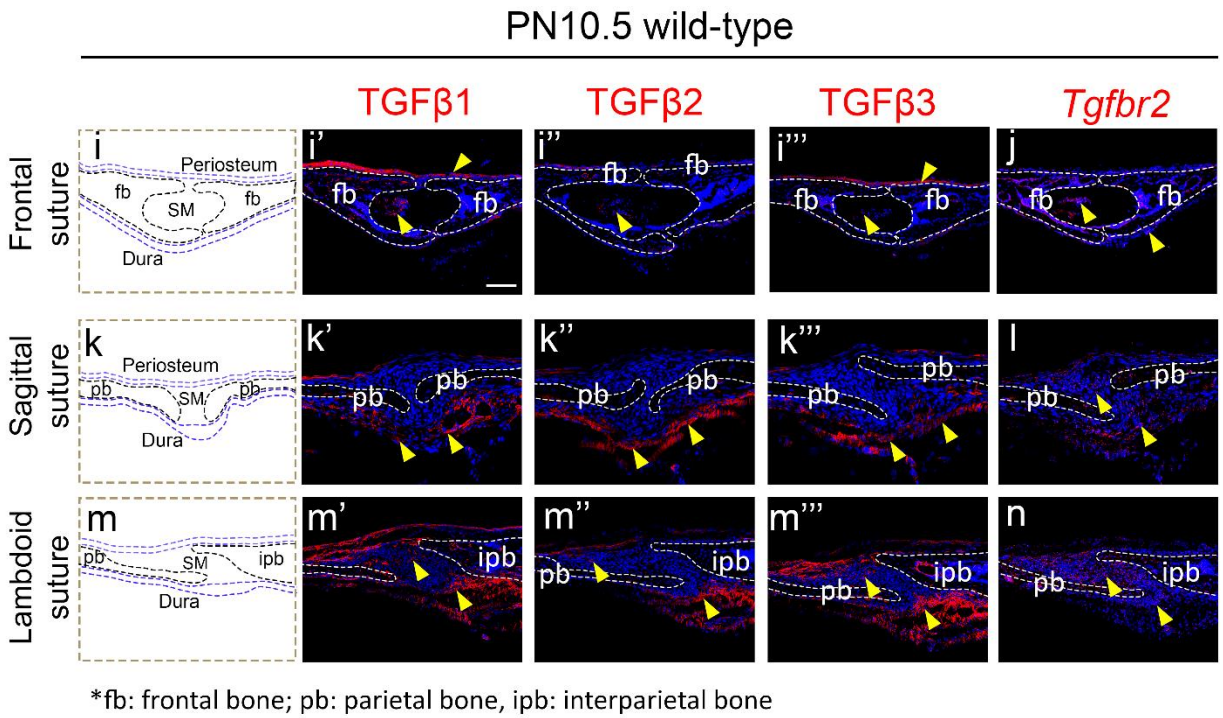


**Supplementary Fig. 7: Loss of *Tgfbr2* in Gli1+ progenitor cells does not lead to frontal, sagittal, or lambdoid suture fusion.**

(i-n) Expression patterns of TGFβ ligands and *Tgfbr2* in different cranial sutures at PN10.5. (i, k, m) Schematic illustrations of the frontal, sagittal, and lambdoid sutures, respectively, indicating periosteum, suture mesenchyme (SM), underlying dura, and adjacent bones. Fb: frontal bone, pb: parietal bone, ipb: interparietal bone. (i'-j) Immunofluorescence staining of TGFβ1, TGFβ2, and TGFβ3, and RNAscope staining of *Tgfbr2* in the frontal suture at PN10.5. (k'-l) Corresponding staining in the sagittal suture. (m'-n) Corresponding staining in the lambdoid suture. White dashed lines outline the bone edges. Yellow arrowheads indicate regions with positive signals. Nuclei are counterstained with DAPI. Scale bar: 100 μm.

**3. The suture allograft in Figure 4 provides vital evidence for dural cells not migrating into the suture without TGFb signaling, resulting in suture fusion. However, additional controls are needed to support this conclusion fully. First, the authors need to transplant other WT sutures (sagittal or lamboid) into the control and mutant recipients. If the authors' hypothesis is correct, tdT+ cells should not migrate into the suture even in the control**

**recipient. Also, the authors should transplant the donor suture into other sutures (either sagittal or lamboid) of the recipient mice. These additional experiments will provide more solid evidence for the specific requirement of TGFb signaling in the coronal suture in an allograft setting.**

We really appreciate the reviewer's suggestion regarding the functional importance of TGFβ signaling in regulating dura cell migration during postnatal suture development. We have added a set of transplant experiments as suggested by the reviewer. To determine whether the migration of dura cells is a universal phenomenon in all sutures, we transplanted PN3.5 WT coronal, sagittal, and lambdoid sutures into the corresponding sutures of *Gli1-Cre$^{ERT2}$;tdT$^{fl/+}$* mice (PN4W) in which dura cells are labeled by tdT. We found that migration of dura cells into mesenchyme could be observed in coronal and lambdoid sutures, as indicated by tdT+ signals, but not in the sagittal suture. Significantly, more dura-derived cells were observed in the coronal suture (**Fig. 2, lines 120-145**), suggesting migration of dura cells may have a more significant role in this suture. Furthermore, to address whether TGFβ signaling regulates dural cell migration in other cranial sutures. We performed additional transplantation experiments using the suture allograft model in both *Tgfbr2$^{fl/fl}$* and *Gli1-Cre$^{ERT2}$;Tgfbr2$^{fl/fl}$* recipients, with the dura labeled by DiI (**Fig. 5l-u, lines 268-280**). Consistent with our original findings, deletion of *Tgfbr2* in *Gli1+* progenitor cells markedly reduced dural cell migration into the coronal suture mesenchyme following coronal suture transplantation. In contrast, when the coronal suture was transplanted into the lambdoid dural environment, or when the lambdoid suture was transplanted into the coronal dural environment, dural cell migration was not significantly affected by *Tgfbr2* deletion (**Fig. 5l-u**). These additional experiments indicate that while dural cell migration can occur in other cranial sutures to some extent, its dependence on TGFβ signaling is most pronounced in the coronal suture environment.

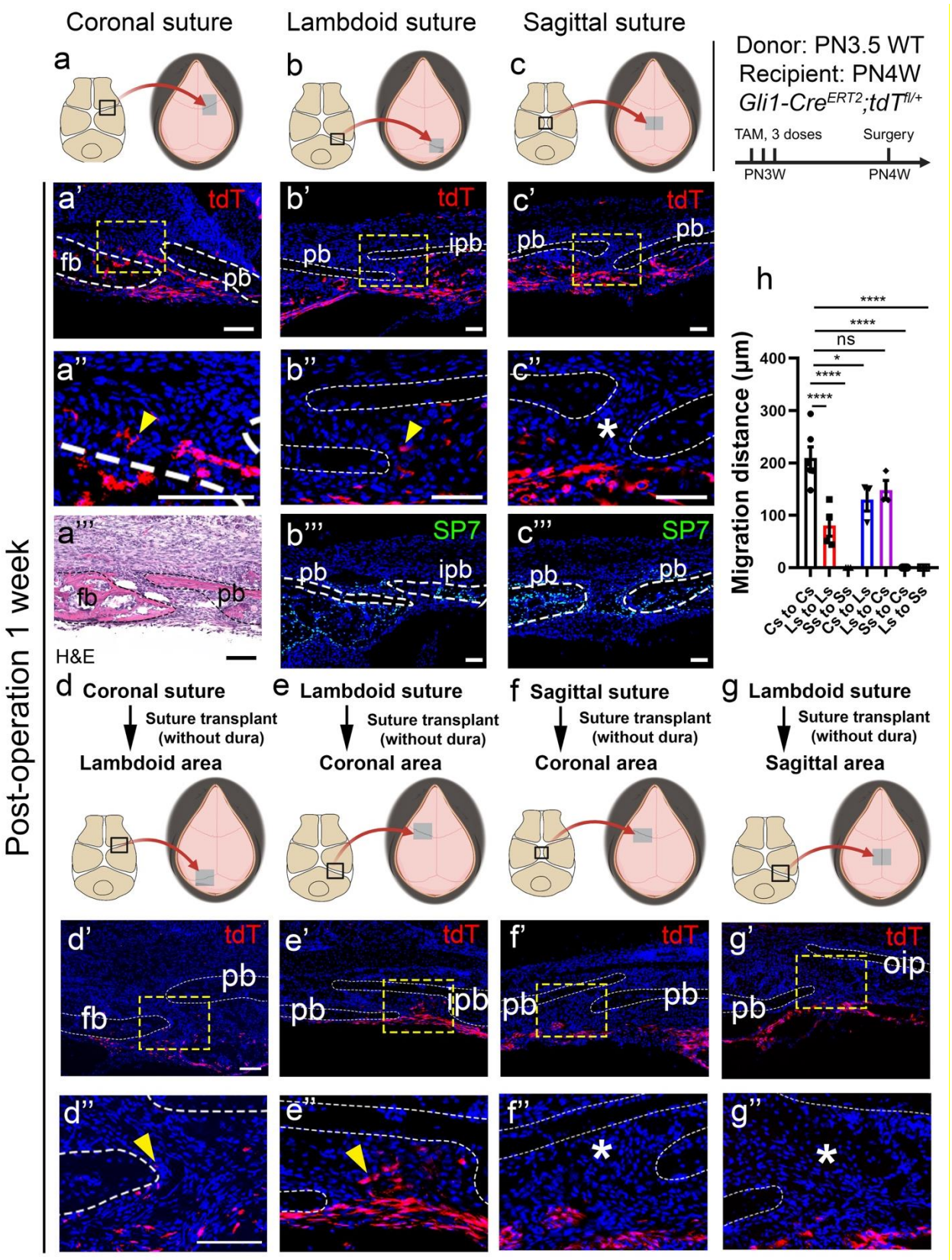


pb: parietal bone; ipb: interparietal bone; fb: frontal bone. All abbreviations indicate donor structures.

**Fig. 2: Dural cell migration is predominantly a coronal suture-specific phenomenon**

(a-c) Schematic drawings showing the surgical procedure for suture transplantation in each group for a'-c'''. (a'-c') Representative fluorescence imagesshowing dural cell migration following suture transplantation. Coronal (a), lambdoid (b), and sagittal (c) suture transplantation seven days after surgery. Donor suture boundaries are outlined by dashed lines. tdT+ dural cells from *Gli1-Cre$^{ERT2}$;tdT$^{fl/+}$* mice are shown in red, and nuclei are counterstained with DAPI in blue. Yellow dashed boxes indicate regions shown at higher magnification in a''-c''. Scale bars: 50μm. (a''-c'') Enlarged views of a'-c'. Arrowheads indicate tdT+ cells and the asterisk denotes absence of tdT+ cells. Scale bars: 50μm. (a''') H&E staining shows the structure of the donor suture after transplantation surgery. (b'''-c''') SP7 immunostaining images showing the bone surface of the donor suture structure. Scale bars: 50μm. (d-g) Representative fluorescence images showing dural cell migration following reciprocal suture transplantation at PN3.5. Coronal, lambdoid, or sagittal sutures were transplanted onto PN4w *Gli1-Cre$^{ERT2}$;tdT$^{fl/+}$* recipients with tdT labeled dura at the indicated recipient sites. Diagram showing procedures of suture transplantation surgery in each group. (d'-g') Low-magnification images showing different transplanted sutures in different dural environments. Donor suture boundaries are outlined by dashed lines. tdT+ dural cells from *Gli1-Cre$^{ERT2}$;tdT$^{fl/+}$* mice are shown in red and nuclei are counterstained with DAPI in blue. Scale bars: 100 μm. (d''-g'') Higher-magnification views of the boxed regions in d'-g'. Arrowheads indicate tdT+ cells, and asterisks denote absence of migration. Scale bars: 100 μm. (h) Quantification of dural cell migration distance. Data are presented as mean ± SEM. Statistical analysis was performed using one-way ANOVA with multiple comparisons. Coronal suture transplanted onto coronal area (N = 6); lambdoid suture onto lambdoid area (N = 4), $p < 0.0001$, ****; sagittal suture onto sagittal area (N = 3), $p < 0.0001$, ****; coronal suture onto lambdoid area (N = 3), $p = 0.0149$, *; lambdoid suture onto coronal area (N = 3), $p = 0.0781$, ns; sagittal suture onto coronal area (N = 3), $p < 0.0001$, ****; lambdoid suture onto sagittal area (N = 3), $p < 0.0001$, ****. Fb: frontal bone, pb: parietal bone, ipb: interparietal bone.

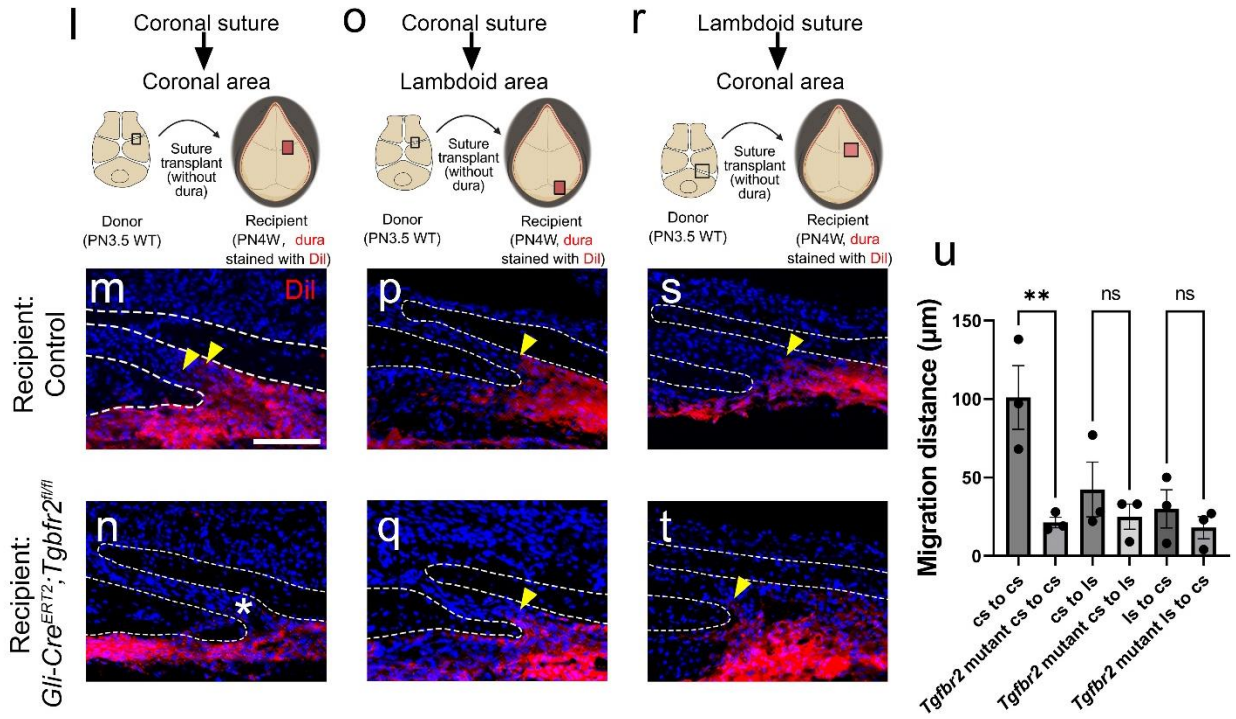


**Fig. 5: Loss of *Tgfbr2* in *Gli1*+ dural cells leads to impaired dural cell migration and subsequently coronal suture fusion.**

(l-u) Dural cell migration following reciprocal suture transplantation using DiI labeled dura. Coronal or lambdoid sutures were transplanted onto control or *Gli1-Cre$^{ERT2}$;Tgfbr2$^{fl/fl}$* recipient mice at the indicated recipient sites. (l-n) Coronal suture transplanted onto the coronal area of control mice (m) or *Gli1-Cre$^{ERT2}$;Tgfbr2$^{fl/fl}$* recipient mice (n). (o-q) Coronal suture transplanted onto the lambdoid area of control mice (p) or *Gli1-Cre$^{ERT2}$;Tgfbr2$^{fl/fl}$* recipient mice (q). (r-t) Lambdoid suture transplanted onto the coronal area in control (s) or *Gli1-Cre$^{ERT2}$;Tgfbr2$^{fl/fl}$* (t) recipients. Donor suture boundaries are outlined by dashed lines. DiI-labeled dural cells are shown in red and nuclei are counterstained with DAPI in blue. Arrowheads indicate migrating dural cells, and an asterisk denotes markedly reduced migration. (u) Quantification of dural cell migration distance in the indicated groups. Data are presented as mean ± SEM. Statistical analysis was performed using one-way ANOVA with multiple comparisons. N = 3 for each group. Coronal suture to coronal area: $p = 0.0089$, ** (control vs. *Tgfbr2* mutant). Coronal suture to lambdoid area: $p = 0.9238$, ns (control vs. *Tgfbr2* mutant). Lambdoid suture to coronal area: $p = 0.9832$, ns (control vs. *Tgfbr2* mutant). Fb: frontal bone, pb: parietal bone, ipb: interparietal bone. Scale bars: 100µm.

**4. The authors should also investigate the potential role of dura-to-suture signals in premature coronal suture fusion. Supplementary Figure 5 shows that the loss of cell proliferation and progenitors occurs acutely upon the loss of Tgfbr2 in Gli1+ cells, long before cell migration occurs, strongly indicating that non-cell-autonomous mechanisms are involved. Mechanisms of premature suture fusion cannot be entirely attributed to defective cell migration. What are the candidates of this dura-to-suture signal? The authors should delve into the RNA-seq datasets, identify potential signaling pathways, and validate the expression patterns using IHC/ISH.**

We thank the reviewer for this insightful comment regarding the potential contribution of dura-to-suture signaling to premature coronal suture fusion. We have analyzed the scRNA-seq datasets to investigate candidate non-cell-autonomous mechanisms (Response letter Fig. 1) and identified several potential signaling pathways, including midkine (MK), thrombospondin (THBS), and FGF signaling. Among these, FGF signaling appears to be the most specifically derived from the dura and functionally relevant to the suture mesenchyme. In particular, the ligand *Fgf18* is highly expressed in the dura and periosteum, whereas its receptors (*Fgfr1-3*) are expressed in the suture mesenchyme, supporting a dura-to-suture paracrine FGF signaling mechanism that may contribute to premature coronal suture fusion.

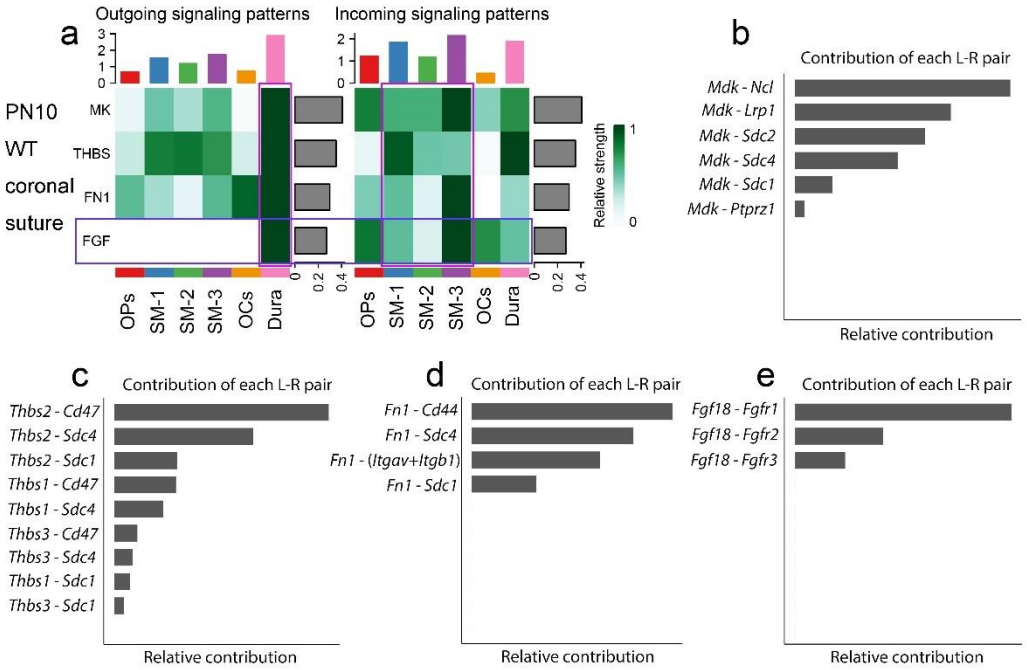


PN10 mice coronal suture mesenchyme

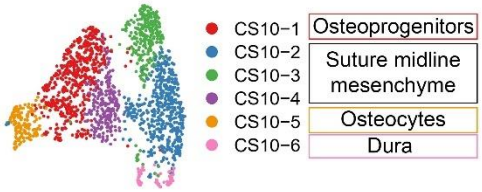


f Ligands

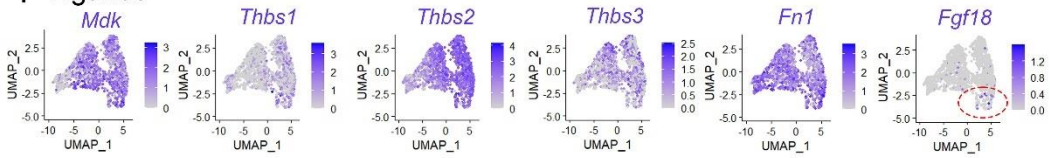


g Receptors

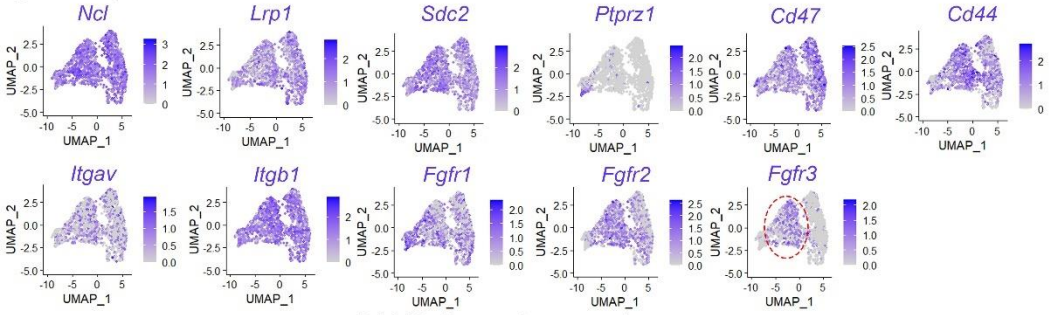


PN10 Control coronal suture

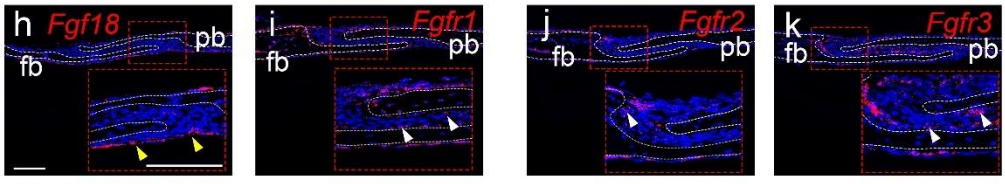


*fb: frontal bone; pb: parietal bone

**Response letter Fig. 1: CellChat analysis showing other signaling pathways that mediate dura-to-suture regulation.**

(a) Heatmaps showing outgoing (left) and incoming (right) signaling patterns among indicated cell populations in the PN10 wild-type coronal suture, as inferred by CellChat analysis. Signaling pathways including midkine (MK), thrombospondin (THBS), fibronectin 1 (FN1), and fibroblast growth factor (FGF) are highlighted. Color intensity indicates relative signaling strength. (b-e) Bar plots showing the relative contributions of individual ligand-receptor (L-R) pairs in the MK (b), THBS (c), FN1 (d), and FGF (e) signaling pathways. (f) UMAP plots showing the expression patterns of selected ligands (*Mdk*, *Thbs1*, *Thbs2*, *Thbs3*, *Fn1*, *Fgf18*) across cell populations in the PN10 coronal suture. (g) UMAP plots showing the expression of corresponding receptors (*Ncl*, *Lrp1*, *Sdc2*, *Ptprz1*, *Cd47*, *Cd44*, *Itgav*, *Itgb1*, *Fgfr1*, *Fgfr2*, *Fgfr3*). (h-k) Representative immunostaining images showing the *in vivo* expression of *Fgf18* (h), *Fgfr1* (i), *Fgfr2* (j), and *Fgfr3* (k) in the PN10 coronal suture. Red dashed boxes highlight regions of enrichment. Dotted lines outline the suture mesenchyme. Nuclei are counterstained with DAPI (blue).

**5. The manuscript lacks the details regarding ex vivo calvarial organ culture, which provides key evidence that dural cells migrate into the coronal suture. How were sutures and dura separated, stained separately, and recombined? There is a technical concern that Q-tracker dyes diffuse the tissue boundaries and stain suture cells without cell migration. The authors should confirm the validity of this approach by genetic marking, using a nuclear fluorescent reporter that does not diffuse across tissue.**

We thank the reviewer for this important comment. Upon further evaluation, we concluded that the *ex vivo* calvarial organ culture system may not adequately recapitulate the *in vivo* suture niche. Therefore, we replaced the organ culture experiments with *in vivo* suture transplantation assays to more faithfully recapitulate physiological conditions. First, we tested several dyes and identified a membrane-labeling dye, Vybrant™ DiI Cell-Labeling Solution (Thermo Fisher, V22885), that effectively labels dural cells without apparent diffusion across tissue boundaries. In our transplantation surgery, calvarial bone containing the suture was gently elevated with fine forceps, allowing separation of the bone from the underlying dura mater while carefully avoiding damage to the dura in donor and recipient mice (**Response letter Fig. 2a**). Following this separation, only the recipient dura was stained with DiI. Then, the donor calvarial bone containing the suture was

placed directly onto the exposed recipient dura at the anatomical location of the recipient suture (**Response letter Fig. 2b**). Using this DiI labeling method, we observed dural cell migration into the coronal suture in a suture transplantation model (**Fig. 1h-k**). In parallel, we also transplanted WT suture mesenchyme into *Gli1-Cre$^{ERT2}$;tdT* recipients. Consistent with DiI labeling, we also observed migration of tdT+ dural cells into the coronal suture mesenchyme (**Fig. 2a-c**).

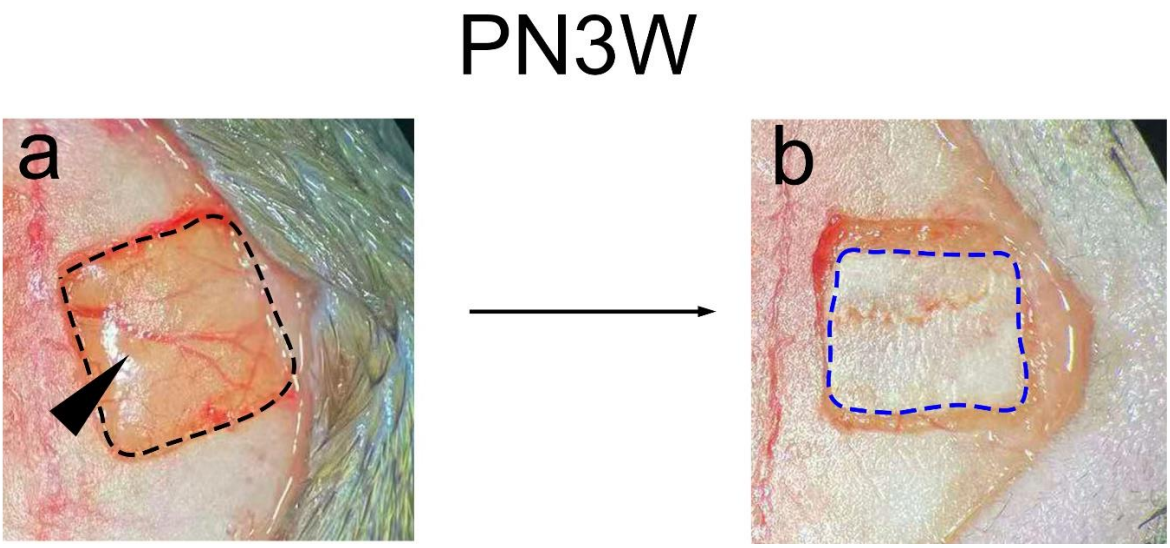


**Response letter Fig. 2: Suture transplantation surgery procedure.**

(a) Exposure of the PN3W dura for suture transplantation. The cranial suture region of PN3W recipient mice was exposed by carefully removing the overlying calvarial bone while preserving the underlying dura mater. The dura remained intact and served as the recipient surface for transplantation. The black dashed lines indicate the region from which the calvarial bone was removed. Arrowhead indicates the exposed dura mater. (b) Transplantation of PN3.5 donor suture onto PN3W dura. The PN3.5 cranial suture, together with adjacent cranial bone segments, was placed onto the exposed dura mater of PN3W recipient mice at the corresponding anatomical location. The graft was aligned along the anterior-posterior axis of the suture to ensure proper orientation. The blue dashed line outlines the donor suture in its transplanted location.

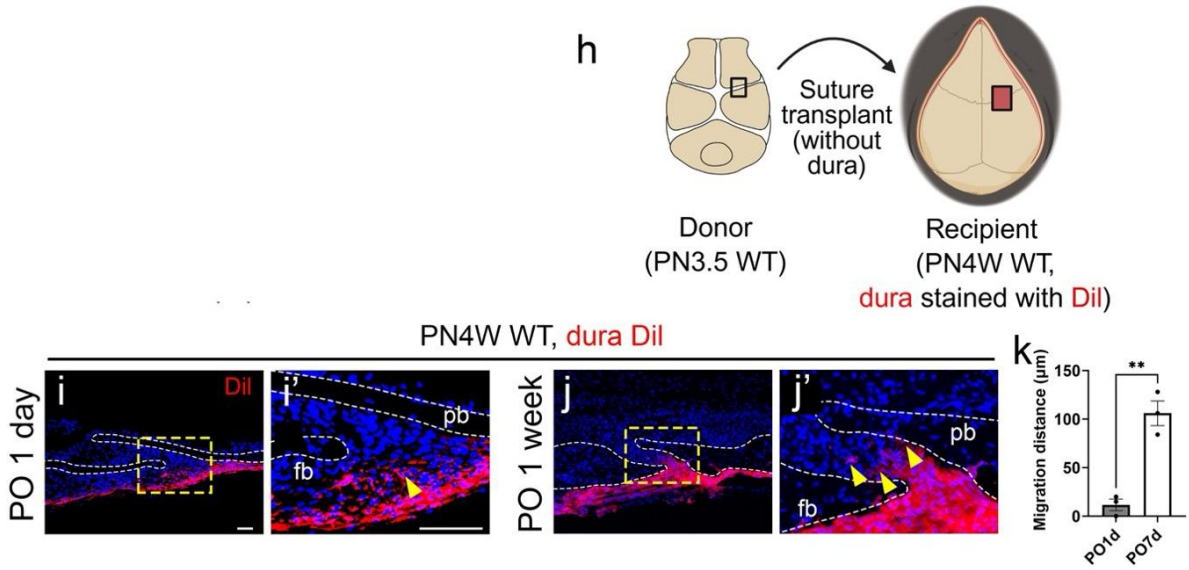


**Fig. 1: Dural cell migration to coronal suture mesenchyme during postnatal development.**

(h-k) Suture transplant model showing dural cells actively migrating into coronal suture mesenchyme. (h) Schematic drawing of suture transplantation surgery. (i) Fluorescence images showing dural cells labeled with DiI (yellow arrowheads) 1 day after suture transplantation surgery. (i') shows the enlarged image from the yellow frame in (i). (j) Fluorescence images showing DiI+ signals (yellow arrowheads) in both the dura mater and suture mesenchyme 7 days after surgery. (j') shows the enlarged image from the yellow frame in (j). (k) Quantitative data in (i', j') are presented as mean ± SEM, $p = 0.0026$, **, calculated by two-tailed unpaired t-test, Scale bar: 50 μm.

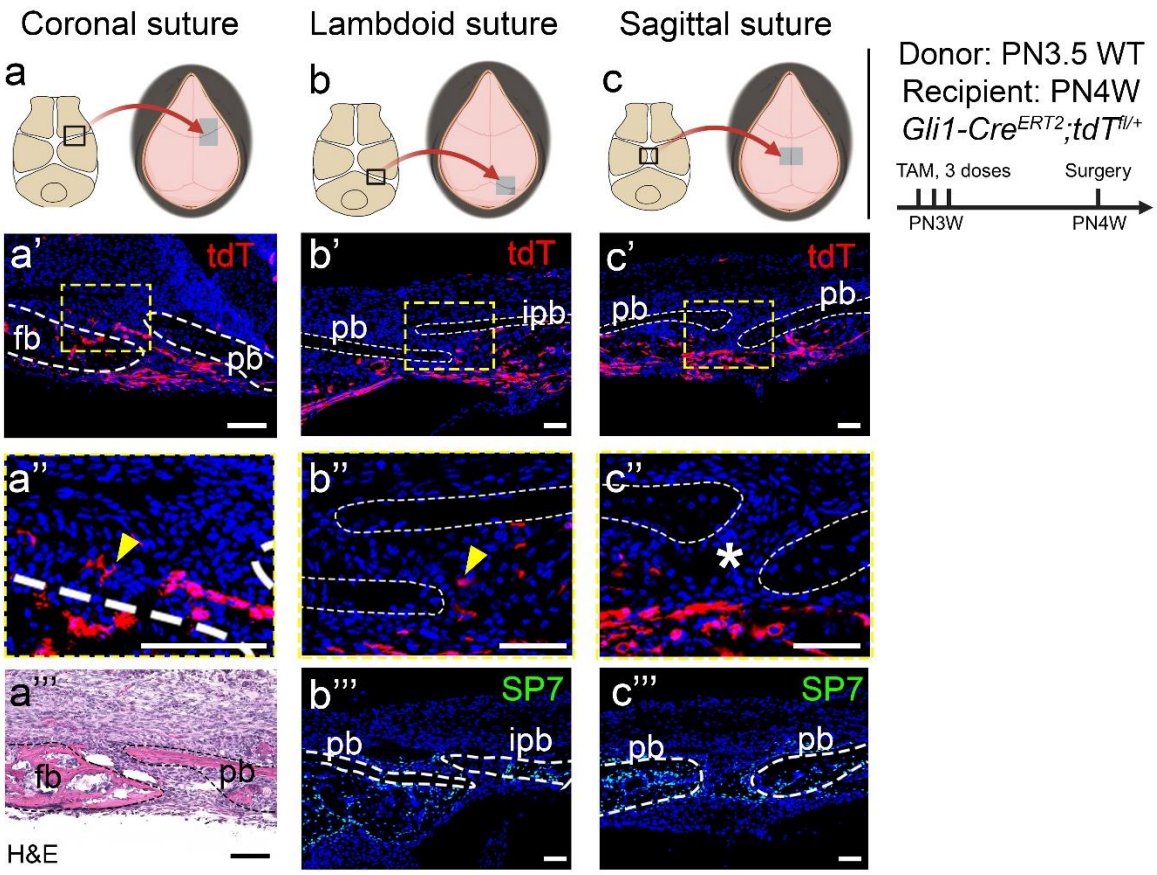


**Fig. 2: Dural cell migration is predominantly a coronal suture-specific phenomenon**

(a-c) Schematic drawings showing the surgical procedure for suture transplantation in each group for a'-c'''. (a'-c') Representative fluorescence imagesshowing dural cell migration following suture transplantation. Coronal (a), lambdoid (b), and sagittal (c) suture transplantation seven days after surgery. Donor suture boundaries are outlined by dashed lines. tdT+ dural cells from *Gli1-Cre$^{ERT2}$;tdT$^{fl/+}$* mice are shown in red, and nuclei are counterstained with DAPI in blue. Yellow dashed boxes indicate regions shown at higher magnification in a''-c''. Scale bars: 50μm. (a''-c'') Enlarged views of a'-c'. Arrowheads indicate tdT+ cells and the asterisk denotes absence of tdT+ cells. Scale bars: 50μm. (a''') H&E staining shows the structure of the donor suture after transplantation surgery. (b'''-c''') SP7 immunostaining images showing the bone surface of the donor suture structure. Scale bars: 50μm. Fb: frontal bone, pb: parietal bone, ipb: interparietal bone.

**6. How does decorin inhibit TGFb in the coronal suture? Does decorin sequester TGFb in the ECM, or does it bind to the receptor? The authors should examine if decorin directly binds to TGFb in the suture by immunohistochemical approaches, such as colocalization.**

We appreciate the reviewer's helpful suggestion. To examine whether decorin interacts with TGFβ ligands in the coronal suture, we co-immunostained decorin and TGFβ1-3 in the suture tissue (Response letter Fig. 3) and observed co-localization of decorin and TGFβ signals in the intercellular space between DAPI-stained nuclei, consistent with their reported interaction within the extracellular matrix of the coronal suture[1]. Moreover, in *Twist1*$^{+/-}$ mice, in which decorin expression is elevated, the extent of decorin-TGFβ colocalization in the intercellular space between DAPI-stained nuclei was increased, indicating that elevated decorin could sequester TGFβ ligands in the extracellular matrix and thereby attenuate TGFβ signaling in the *Twist1*$^{+/-}$ mice.

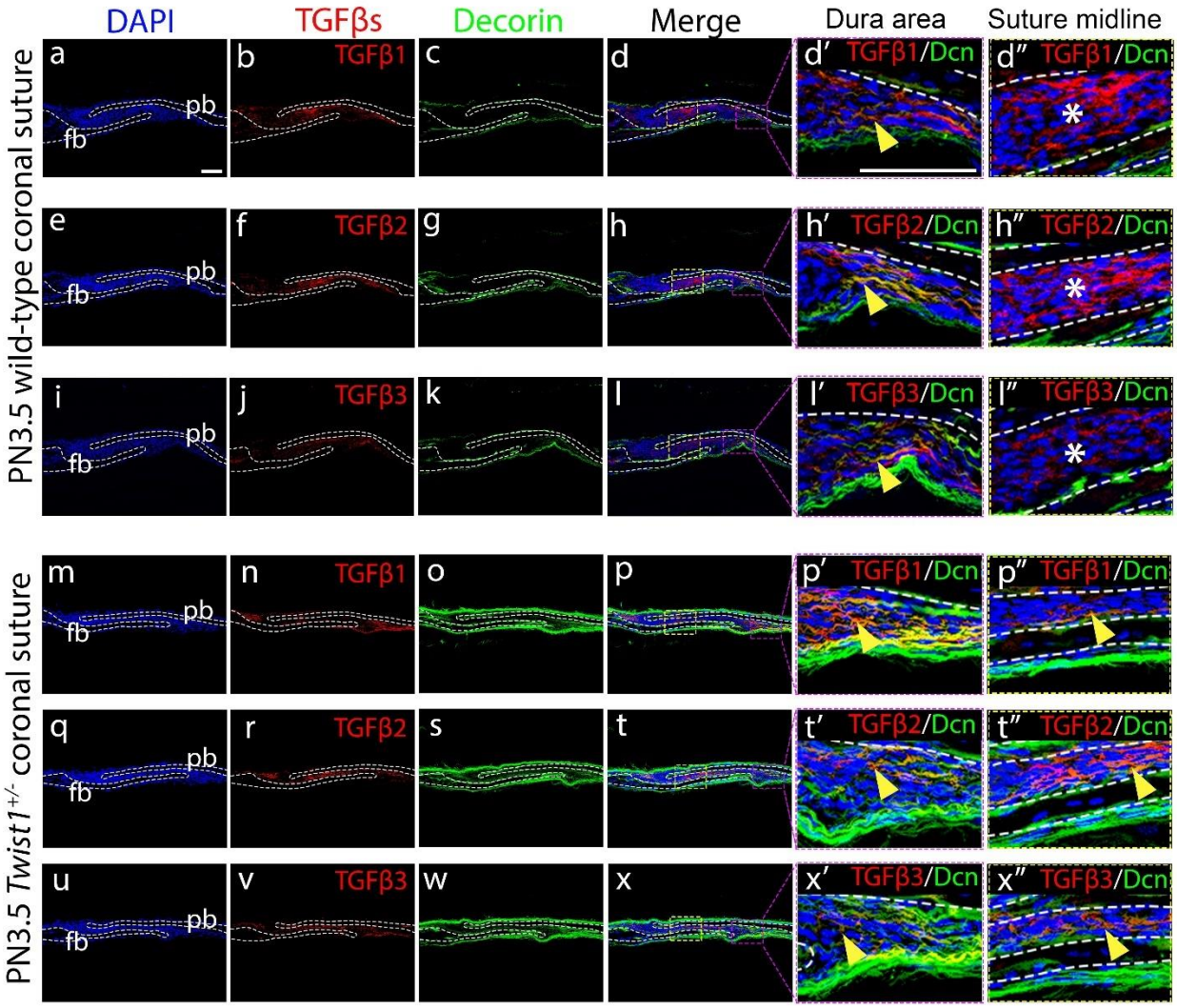


**Response letter Fig. 3: Co-localization of TGFβ ligands and decorin in wild type and *Twist1*$^{+/-}$ coronal sutures at PN3.5.**

Immunofluorescence co-staining of TGFβ1, TGFβ2, and TGFβ3 with decorin in wild type (a-l) and *Twist1*$^{+/-}$ (m-x) coronal sutures at PN3.5. DAPI marks nuclei. White dashed lines outline the bone edges. fb frontal bone, pb parietal bone. High magnification views of the dura region are shown in d', h', l', p', t', and x'. High magnification views of the suture midline are shown in d'', h'', l'', p'', t'', and x''. Yellow arrowheads indicate regions of TGFβ and decorin co-localization. Asterisks indicate the absence of co-expression. Scale bars: 100 μm.

**7. A dura-specific marker (such as Rbp1/RBP1) should be used to demonstrate the localization of some important readouts, such as Q-tracker, Tgfbr2, and Gli1-tdT.**

We thank the reviewer for this helpful suggestion. To better define the localization of dural cells in our studies, we performed co-immunostaining of RBP1, a dura-specific marker, with Gli1-tdT and *Tgfbr2*. We confirmed that tdT+ cells are colocalized with RBP1+ cells in the dura (**Fig. 5 b-b''**), and *Tgfbr2* is co-expressed in the RBP1+ dura (**Fig. 4a-a'''**).

For DiI-labeled sections, however, co-staining with RBP1 was technically challenging because the tissue processing required for RBP1 immunostaining diminished the DiI signal. Since DiI was applied to the dural side and the signal was anatomically restricted to the dural layer (**Fig. 1i,j**), we used this anatomical specificity to confirm labeling specificity.

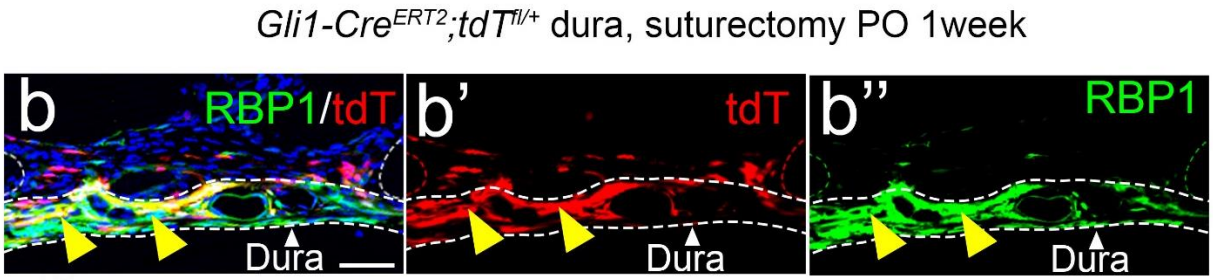


**Fig. 5: Loss of *Tgfbr2* in *Gli1*+ dural cells leads to impaired dural cell migration and subsequently coronal suture fusion.**

(b) Immunofluorescence images showing tdT+ signals (red) co-stained with dura marker RBP1 (green) one week after suturectomy surgery. Yellow arrowheads indicate positive co-expression signals.

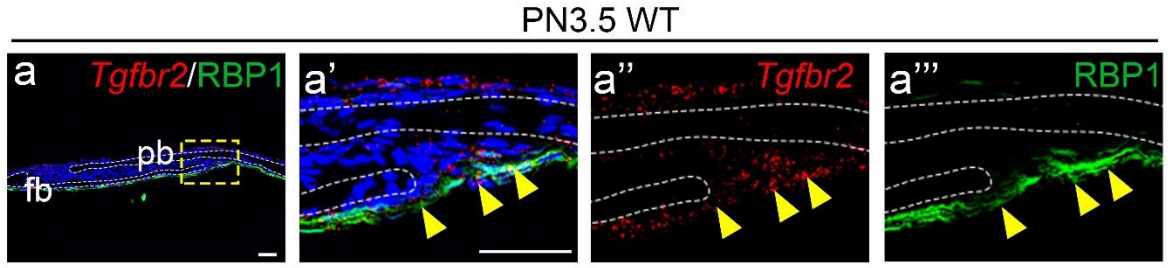


**Fig. 4: Loss of *Tgfbr2* in *Gli1+* progenitor cells leads to coronal suture fusion.**
(a) Double staining of the coronal suture region in PN3.5 WT mice showing *Tgfbr2* (red) and RBP1 (green), with the boxed region shown enlarged in (a'-a'''). Merged image (a') demonstrates clear co-expression of RBP1 and *Tgfbr2* in the dura (yellow arrowheads). Dashed lines outline tissue boundaries. Scale bars: 50 μm.

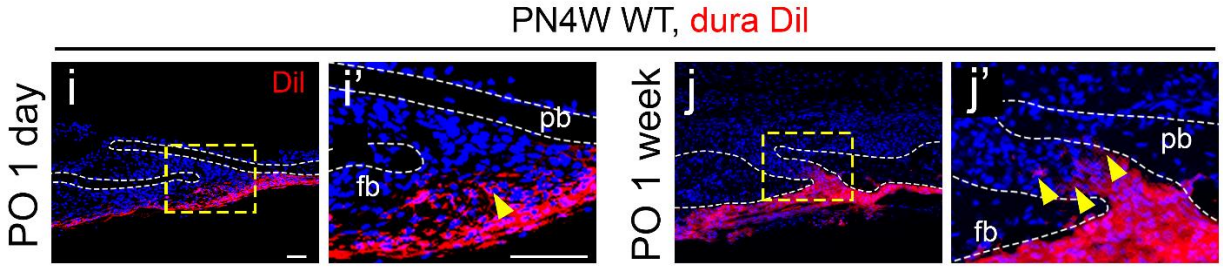


**Fig. 1: Dural cell migration to coronal suture mesenchyme during postnatal development.** (i) Fluorescence images showing dural cells labeled with DiI (yellow arrowheads) 1 day after suture transplantation surgery. (i') shows the enlarged image from the yellow frame in (i). (j) Fluorescence images showing DiI+ signals (yellow arrowheads) in both the dura mater and suture mesenchyme 7 days after surgery. (j') shows the enlarged image from the yellow frame in (j). Scale bars: 50 μm.

**The individual points are described below.**

**Individual points:**

**8. Abstract - Line 33: The authors should clarify that decorin is upregulated in Twist mutant mice, which leads to dampened TGFb signaling.**

We thank the reviewer for this helpful suggestion. We have revised the Abstract to explicitly state that decorin is upregulated in *Twist1* mutant mice and that this upregulation is associated with reduced TGFβ signaling activity. The revised text reads: "Furthermore, in *Twist1*$^{+/-}$ mice recapitulating human Saethre-Chotzen syndrome, upregulated decorin leads to compromised TGFβ signaling, which impairs dural cell migration, leading to craniosynostosis."

**- Line 34: The authors did not really show the data that "restoring TGFb signaling rescues coronal suture patency in Twist1+/- mice". It is only decorin inhibition by shRNA that rescued the phenotype. The authors should be explicit about this.**

We thank the reviewer for this comment. We have included data showing that inhibition of decorin by shRNA in *Twist1*$^{+/-}$ sutures led to a marked increase in p-SMAD2 levels (**Revised Fig. 7j-n**), indicating restoration of TGFβ signaling activity. This restoration of TGFβ signaling was associated with rescue of coronal suture patency, supporting a link between decorin-mediated attenuation of TGFβ signaling and suture fusion in the *Twist1*$^{+/-}$ mice.

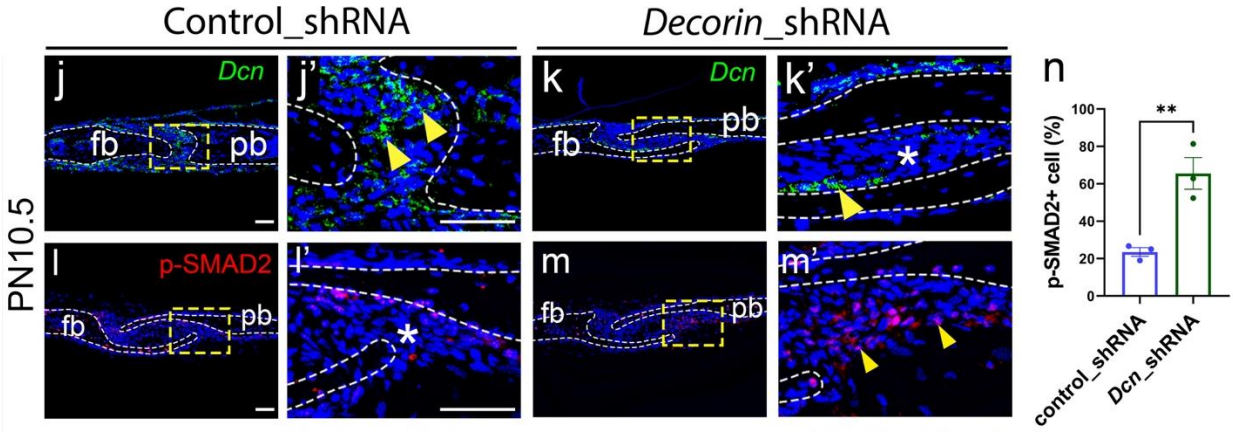


**Fig. 7: Decorin overexpression induces coronal suture fusion and its inhibition restores patency in *Twist1*$^{+/-}$ mice.**

(j-k) RNAscope staining showing *Dcn* knockdown in the coronal suture mesenchyme of *Twist1*$^{+/-}$ mice. (j, j') *Dcn* expression at PN10.5 in the control_shRNA-treated group. (k, k') Reduced *Dcn* expression in the suture mesenchyme (asterisk) after *Dcn* knockdown. Panels j' and k' show magnified views of the yellow boxed regions in j and k, respectively, with yellow arrowheads indicating *Dcn*-positive signals. Scale bar: 50 μm. (l-n) Immunofluorescence staining showing restored p-SMAD2 levels in *Dcn*_shRNA-treated *Twist1*$^{+/-}$ mice (m-m') compared to those treated

with control_shRNA (l-l'). Panels l' and m' show magnified views of the yellow boxed regions in (l) and (m), respectively, with yellow arrowheads indicating positive signals. Asterisk indicates absence of signal. (n) Quantitative data are presented as mean ± SEM, $p$ = 0.0088, **, N = 3, calculated by two-tailed unpaired t-test. Scale bars: 50 μm.

**- Line 36: As mentioned above, it is not only dural cell migration that contributes to coronal fusion. A dura-to-suture signal appears to be involved as well. The authors should remain open to this possibility.**

We thank the reviewer for this statement of caution. We have revised the Abstract and rephrased the text to "These findings identify the critical role of TGFβ-mediated dural-suture interactions, particularly dural cell migration, in maintaining coronal suture patency and provide an explanation for the preferential coronal fusion in syndromic craniosynostosis."

**9. Introduction**

**- Lines 70-73: The authors should mention decorin upregulation as a mechanism for impaired TGFb signaling.**

We appreciate this suggestion. We have added a statement in the introduction to the effect that upregulation of decorin leads to reduced TGFβ signaling. The revised text reads: "In the highly clinically relevant *Twist1*$^{+/-}$ mouse model with coronal suture fusion, *Twist1* haploinsufficiency results in upregulation of decorin, which impairs TGFβ signaling and leads to reduced dural cell recruitment into the suture."

**10. Results**

**- Lines 85-86: Figure 1b. The authors should use a dura-specific marker to highlight the structure. The distinction between the frontal bone and the dura mater is obscure.**

We thank the reviewer for this helpful suggestion. To clarify the distinction between the frontal bone and the dura mater, we performed RNAscope staining for the dura-specific marker *Rbp1*. The *Rbp1* staining clearly delineates the dural layer from the adjacent frontal bone and is provided below for reference (Response letter Fig. 4).

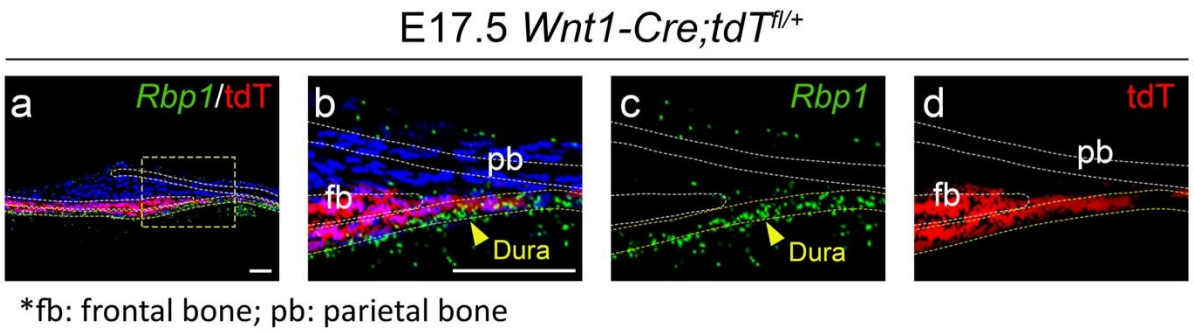


**Response letter Fig. 4: *Rbp1* marks the dura and colocalizes with Wnt1-tdT+ cells.**

(a-d) RNAScope staining of *Rbp1* (green) and Wnt1-tdT (red) in the E17.5 coronal suture region. *Rbp1* expression specifically labels the dura, and tdT+ cells are localized within the same dural layer, showing colocalization in the dura (yellow arrowheads). Boxed regions in (a) are shown at higher magnification in (b-d). Nuclei are stained with DAPI (blue). fb, frontal bone; pb, parietal bone. Scale bar: 100 μm.

**- Lines 89-91: Figure 1c-f. The authors quantify the number of tdT+ cells in the suture mesenchyme across biological replicates and provide a graph.**

We appreciate this suggestion and have added this quantification in revised Fig. 1g.

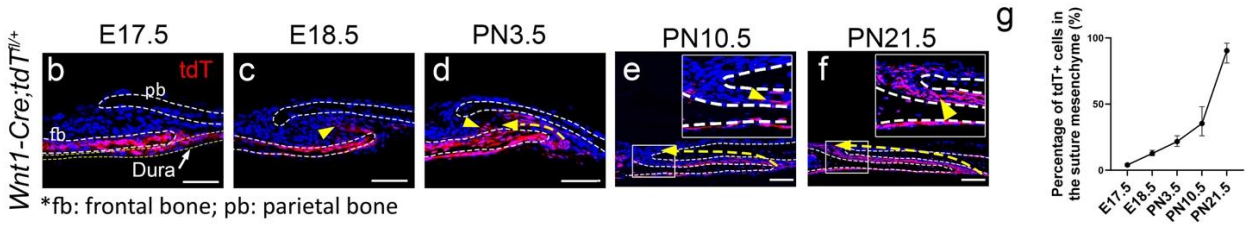


**Fig. 1: Dural cell migration to coronal suture mesenchyme during postnatal development.**

(b-f) The dynamic change in coronal suture neural crest-derived cells (labeled by tdT) over time during coronal suture development. (g) Temporal trend of tdT+ cell percentage within the coronal suture mesenchyme. Yellow arrowheads show the tdT+ signals; yellow dashed lines show the potential migration trajectory. Scale bars: 50 μm.

**- Lines 98-99: The authors should explain in detail in the main text how the ex vivo organ culture model was performed, and how a dye stained the underlying dura. A dura-specific marker should also confirm the validity of dye staining. (After marker)**

We thank the reviewer for this suggestion. As described above, we have replaced the *ex vivo* organ culture model with an *in vivo* transplantation experiment using DiI, which more closely recapitulates *in vivo* conditions. However, co-staining with RBP1 was technically challenging because the tissue processing required for RBP1 immunostaining diminished the DiI signal. Since DiI was applied to the dural side and the signal was anatomically restricted to the dural layer (Fig. 1i, j), we used this anatomical marker to confirm labeling specificity.

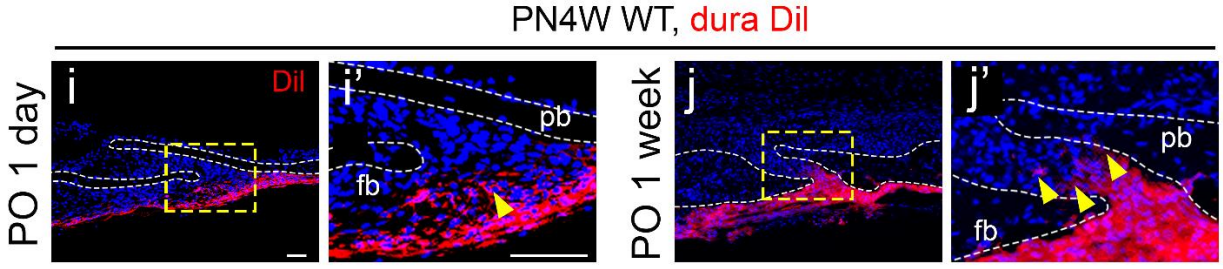


**Fig. 1: Dural cell migration to coronal suture mesenchyme during postnatal development.**

(i) Fluorescence images showing dural cells labeled with DiI (yellow arrowheads) 1 day after suture transplantation surgery. (i') shows the enlarged image from the yellow frame in (i). (j) Fluorescence images showing DiI+ signals (yellow arrowheads) in both the dura mater and suture mesenchyme 7 days after surgery. (j') shows the enlarged image from the yellow frame in (j). Scale bars: 50 μm.

**- Line 111-112: According to Figure 1d, it is not only the frontal bone cells that were genetically labeled by ZsGreen. Some of the suture mesenchymal cells are also marked. The authors should clarify.**

We thank the reviewer for this comment. We agree that, as shown in Figure 1d, ZsGreen labeling is not restricted exclusively to frontal bone cells. At PN3.5, a small population of Wnt1-ZsGreen+ cells is already present within the suture mesenchyme (Fig. 1o), consistent with early postnatal neural crest contribution. We have now clarified this point in the Results section (**lines 112-114**) to avoid confusion and to explicitly note the presence of ZsG+ cells within the suture mesenchyme

at this developmental stage. The revised text reads: “We also noted that, at PN3.5, a small subset of ZsG+ cells was already present within the suture mesenchyme (Fig. 1n-o), consistent with early postnatal neural crest contribution (Fig. 1d).”

**- Line 175-176: Figure 3e-j. The authors should clarify how many biologically independent animals they examined and describe the penetrance of the phenotype. Did all the mutant mice show craniosynostosis specifically in the coronal suture? Did the authors look at both male and female mice?**

We appreciate the opportunity to clarify. In Fig. 3e-j, we analyzed four biologically independent pairs of animals. All four mutant mice exhibited craniosynostosis specifically in the coronal suture. Both sexes were examined, including two female and two male mice. This information has been added to the legend of **revised Fig. 4**.

**- Lines 213-216: The authors should clarify if these results were observed across biological replicates.**

We thank the reviewer for this comment. These results were observed across 4 biological replicates, and we have added this to the Results section (**Lines 209-213**).

**- Lines 220-221: Figure 5d-f. The concern is that Q-tracker can diffuse across tissues, as there are some signals in the frontal and parietal bones.**

Based on reviewer’s suggestion, we have tested another dye (DiI, Vybrant™ DiI Cell-Labeling Solution, ThermoFisher, V22885) that labels cell membrane. DiI nicely labeled the dura and indicated active dural cell migration into the coronal suture in a suture transplantation model (**Fig. 1h-k**). More importantly, we have also added experiments using WT suture mesenchyme transplanted into *Gli1Cre$^{ERT2}$;tdT$^{fl/+}$* recipients. Consistent with the dye labeling, we observed migration of tdT+ dura cells into suture mesenchyme (**Fig. 2a-c**).

**- Lines 283-284: Figure 7d-f. The authors should also inject decorin protein in other sutures (sagittal or lamboid) to examine if it causes partial suture fusion.**

We thank the reviewer for this helpful suggestion. We have performed additional experiments in which recombinant decorin protein was injected into the sagittal and lambdoid suture regions to test whether decorin induces fusion of other sutures. Our observations suggest that decorin

treatment does not induce comparable fusion in these sutures, supporting a coronal suture-specific response to decorin treatment. These data are included in the revised manuscript (**lines 326 to 329**) and **Supplementary Fig. 8d-o**.

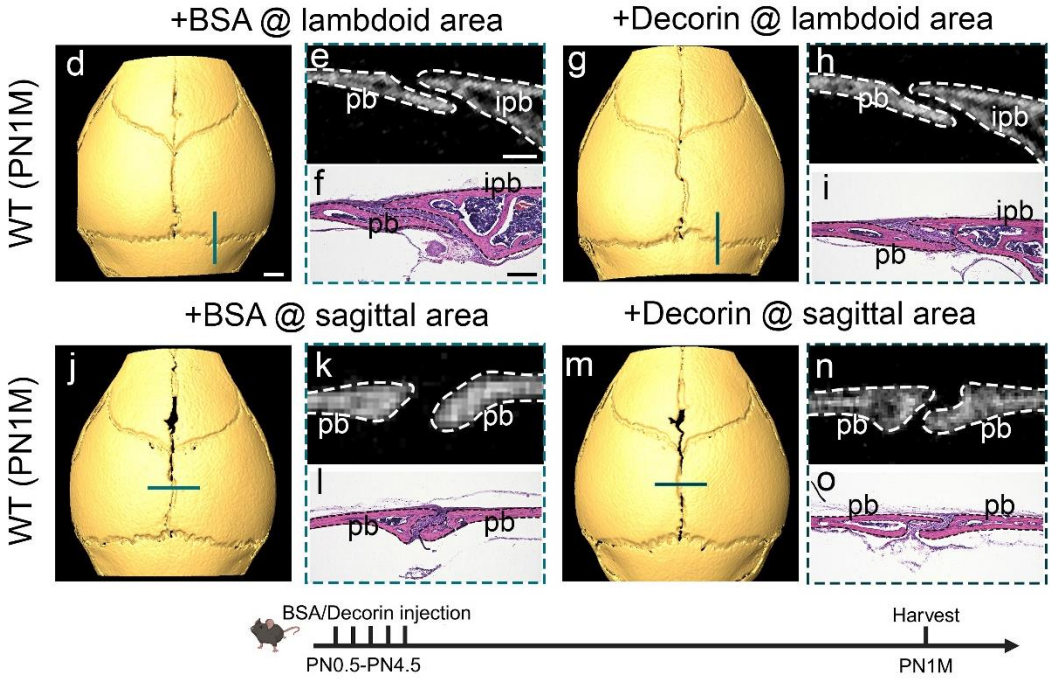


**Supplementary Fig. 8: The function of Decorin in coronal dural cells, lambdoid suture, and sagittal suture.**

(d-o) Representative three-dimensional micro-CT reconstructions and corresponding histological sections of wild-type mouse skulls at PN1M following postnatal injection of BSA or decorin protein into lambdoid or sagittal suture regions. (d-f) BSA injection into the lambdoid suture region did not affect suture patency, as shown by micro-CT imaging (c-d) and H&E staining (e) (N = 3). (g-i) Decorin injection into the lambdoid suture region similarly did not result in suture fusion or narrowing (N = 3). (j-l) BSA injection into the sagittal suture region showed normal sagittal suture patency (N = 3). (m-o) Decorin injection into the sagittal suture region did not induce suture fusion, with preserved suture morphology observed by micro-CT and histological analysis (N = 3). Decorin or BSA was injected daily from PN0.5 to PN4.5, and skulls were harvested at PN1M, N=3 per group. Pb: parietal bone, ipb: interparietal bone. Scale bars: 1mm (d), 200 μm (e-f).

## 11. Materials and Methods

**- Lines 758-768: This section on developing mouse brain volume calculation is irrelevant to the current manuscript.**

We thank the reviewer for pointing this out. The section describing the developing mouse brain volume calculation corresponds to the analysis presented in the Discussion section (Lines 356-359, Supplementary Fig. 9), where we compare developmental brain growth dynamics with cranial suture development. To avoid confusion, we have clarified this connection in the revised manuscript.

**12. Figures**

**- Figure 1g-h: The Q-tracker signal in the suture after organ culture should be quantified across biological replicates.**

We thank the reviewer for this suggestion. We have now quantified DiI-labelled dural cell migration in the suture transplantation model across 3 biological replicates and included it in Fig. 1i-k.

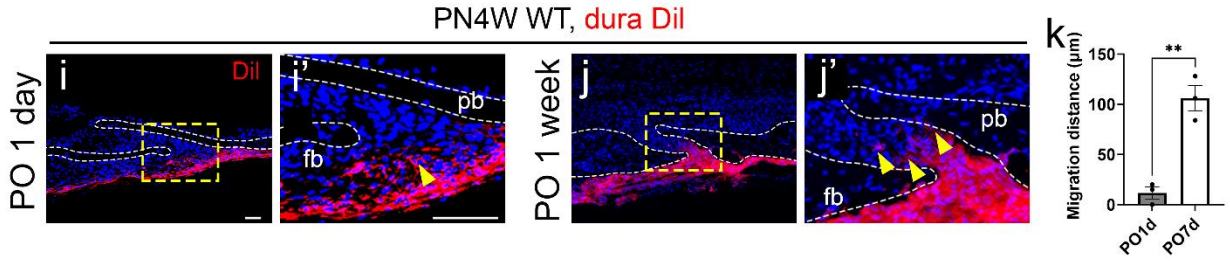


**Fig. 1: Dural cell migration to coronal suture mesenchyme during postnatal development.**

(i-k) Suture transplant model showing dural cells actively migrating into coronal suture mesenchyme. (i) Fluorescence images showing dural cells labeled with DiI (yellow arrowheads) 1 day after suture transplantation surgery. (i') shows the enlarged image from the yellow frame in (i). (j) Fluorescence images showing DiI+ signals (yellow arrowheads) in both the dura mater and suture mesenchyme 7 days after surgery. (j') shows the enlarged image from the yellow frame in (j). (k) Quantitative data in (i', j') are presented as mean ± SEM, $p$ = 0.0026, **, calculated by two-tailed unpaired t-test, Scale bars: 50 μm.

**- Figure 1j-o: The ZsGreen and tdT signals in the suture after allograft should be quantified across biological replicates.**

We thank the reviewer for this suggestion. We have included quantification for the ZsGreen and tdTomato signals within the suture mesenchyme after allografting across biological replicates (**Fig. 1p**). (N = 3)

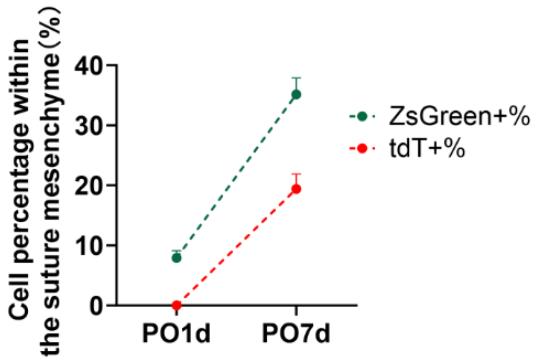


**Fig. 1: Dural cell migration to coronal suture mesenchyme during postnatal development.**

(p) Temporal trends of tdT+ and ZsG+ cell percentage within the coronal suture mesenchyme.

**- Figure 3a-d: The quantification of Tgfbr2 and p-SMAD2 signal is needed.**

We thank the reviewer for this suggestion. We have quantified the *Tgfbr2* and p-SMAD2 signals in Fig. 4f-g across 3 biological replicates, and the corresponding quantitative data with sample sizes are included in **the revised Fig. 4**.

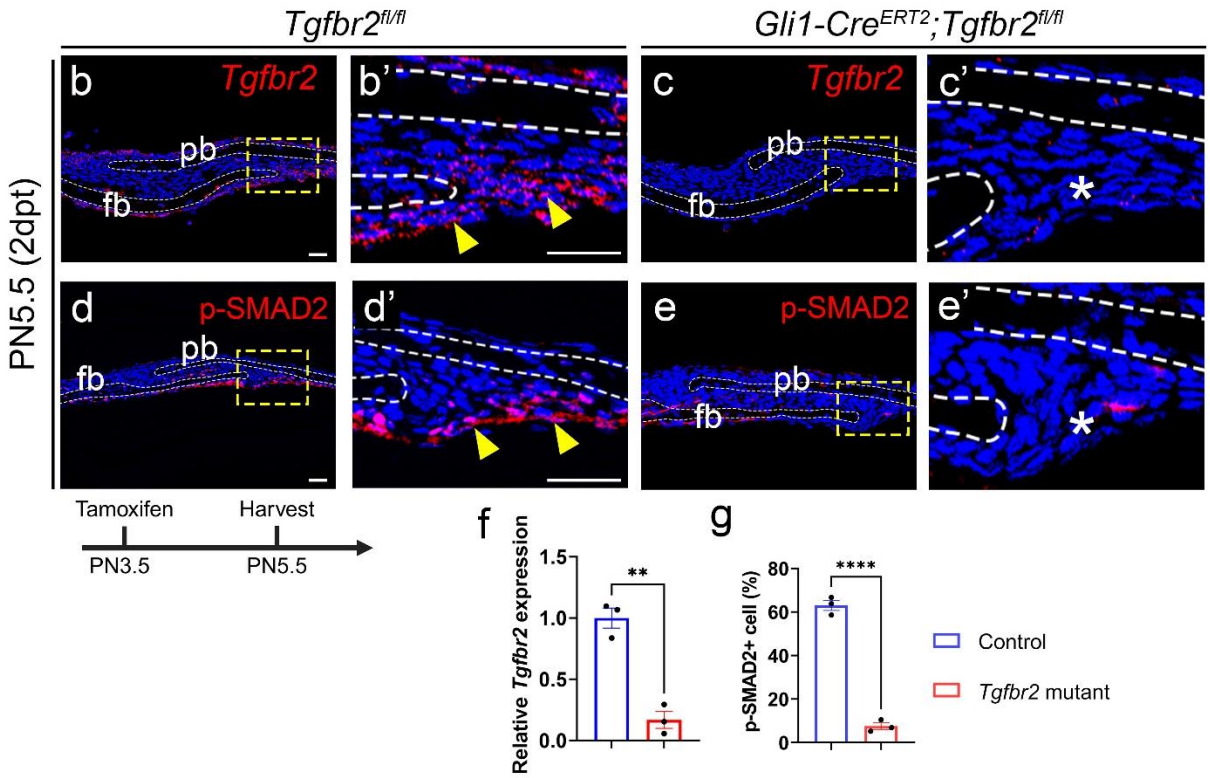


**Fig. 4: Loss of *Tgfbr2* in *Gli1*+ progenitor cells leads to coronal suture fusion.**

(b-c) RNAscope staining showing the efficient deletion of *Tgfbr2* in the coronal suture and dura. (b-b') *Tgfbr2* expression pattern in control mice 2 days post-tamoxifen induction (2dpt). (b') shows a magnified view of the boxed region in (b), with yellow arrowheads indicating that *Tgfbr2* is mainly expressed in the dura. (c-c') In *Gli1-Cre*$^{ERT2}$*;Tgfbr2*$^{fl/fl}$ mice, *Tgfbr2* is efficiently deleted, indicated by the absence of positive signals shown as an asterisk. (c') shows a magnified view of the boxed region in (c). Scale bars: 50 μm. (d-e) Immunofluorescence images showing the reduced p-SMAD2 levels following deletion of *Tgfbr2* in *Gli1*+ progenitor cells. (d-d') p-SMAD2 expression pattern in control mice 2 days post-tamoxifen induction. Yellow arrowheads indicate p-SMAD2 is highly enriched in the dura. (d') shows a magnified view of the boxed region in (c). (e-e') p-SMAD2 expression pattern in *Gli1-Cre*$^{ERT2}$*;Tgfbr2*$^{fl/fl}$ mice. White asterisk indicates absence of positive p-SMAD2 signal. (e') shows a magnified view of the boxed region in (e). Scale bars: 50 μm. (f) Quantitative data in (b-c) are presented as mean ± SEM, calculated by two-tailed unpaired t-test, $p = 0.0015$, **, N = 3. (g) Quantitative data of (d-e) are presented as mean ± SEM, calculated by two-tailed unpaired t-test, $p < 0.0001$, ****, N = 3.

**- Figure 4d-i: The authors should clarify if these results were observed across biological replicates and provide quantification, as appropriate.**

We thank the reviewer for this suggestion. The results shown in Fig. 4d-i were consistently observed across three biological replicates. We have included quantitative analyses for these experiments, and the corresponding data with sample sizes are included in the **revised Fig. 5e-k**.

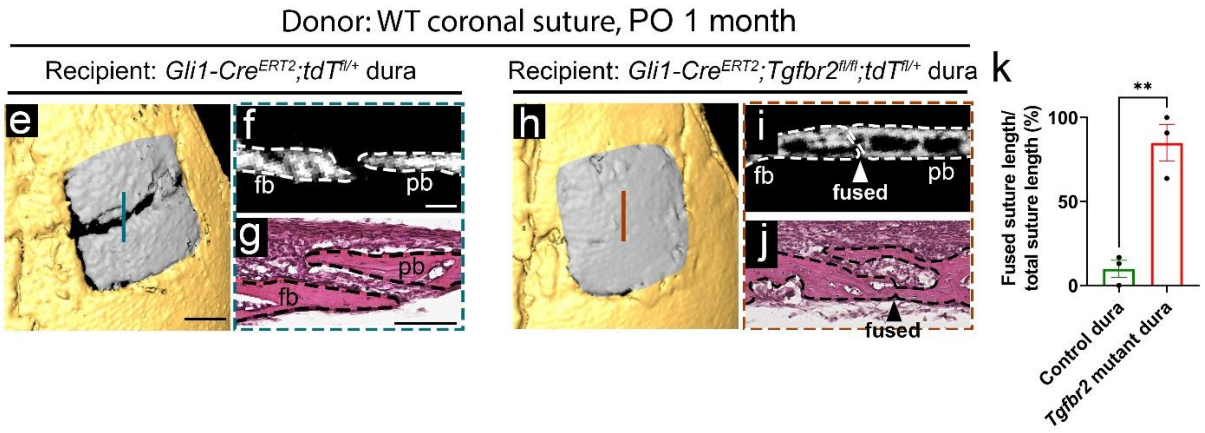


**Fig. 5: Loss of *Tgfbr2* in *Gli1+* dural cells leads to impaired dural cell migration and subsequently coronal suture fusion.**

(e-g) Micro-CT 3D reconstruction (e), CT slice image (f), and H&E staining (g) showing that the transplanted coronal suture remained patent when transplanted onto *Gli1-Cre$^{ERT2}$;tdT$^{fl/+}$* mouse dura. The cyan line in (e) indicates the anatomical location of (f) and (g). Scale bar in (e), 1 mm; other scale bars, 200 μm. (h-j) Micro-CT 3D reconstruction (h), CT slice image (i), and H&E staining (j) showing that the transplanted coronal suture fused when transplanted onto *Gli1-Cre$^{ERT2}$;Tgfbr2$^{fl/fl}$;tdT$^{fl/+}$* mouse dura. The brown line in (h) indicates the anatomical location of (i), (j). (k) Quantitative data in (e, h) are presented as mean ± SEM, calculated by two-tailed unpaired t-test, $p$ = 0.0033, **, N = 3.

**Reviewer #2 (Remarks to the Author):**

**Chen et al. Present a tour de force of developmental biology and genetics that is impressive in its breadth of techniques and convincing mechanistic insights. The authors explore why the coronal suture, as oppose to the other sutures of the skull vault, are differently affected**

**in disease. Although during embryonic stages, the coronal suture is mesoderm-derived, the authors use a genetic reporter to find increasing numbers of neural crest cells in the coronal sutures during postnatal development. The authors find neural crest cells invade the suture from the underlying dural cells specifically in the coronal suture, using in and ex vivo lineage tracing. This invasion is attributed to increased proliferation of DuSCs which then migrate into the coronal suture. Analysis of various sequencing data sets implicated TGFbeta signaling in promoting dural cell invasion. The authors confirmed this link through genetic and chemical abrogation of TGFβ which caused coronal synostosis and reduced dural-derived stem cell invasion. These data were consistent with the reduced TGFβ signaling found in Twist1 mutants which develop coronal synostosis. An inhibitor of TGFβ, Decorin (Dcn), was increased in mutant coronal sutures raising the hypothesis that Dcn limits migration of DuSCs into the suture mesenchyme by modulating TGFβ signaling between suture mesenchyme and the dura. Coronal synostosis and loss of DuSC invasion into the suture was found in Dcn treated animals, confirming a role for Suture-Dura TGFβ signaling in directing DuSCs into the coronal suture mesenchyme. These data provide a beautiful cell biological understanding of suture biology that has significant implications for treating human disease.**

**The manuscript presented by Chen et al. is of very high quality and provides exciting and important intellectual and technical advancements in craniofacial biology and development more broadly. This reviewer is extremely excited by this manuscript and looks forward to its publication, although very minor points should be addressed.**

**1. Ref 20 doesn't seem appropriate as this is not original Mesp1 data and does not show data or illustrations pertaining to the skull. Other publications better show the Mesp1 label at the coronal suture (e.g. Yen et al. 2010, Tabler et al. 2016, Larsen's Human Embryology etc).**

We thank the reviewer for pointing this out. We have added Ref. 21-23 to the reference list to replace Ref. 20 with publications that more directly demonstrate *Mesp1* lineage contribution to the coronal suture.

**2. Ref 18 refers to labelling of dissociated suture cells with Q Tracker performed in previous work from the Chai lab. However, that protocol is quite different from the experiment described here where only exposed cells of the explant take up the Q tracker nanocrystals. It would help to describe the experiment more thoroughly in this manuscript (even if just in the methods) as some may be concerned that the dye is easily incorporated into cells other than the dura. However, the large 2um size of the nanocrystals makes it unlikely that Q-Tracker nanodots will be taken up accept by cells directly exposed to dye-containing media. This should be explicitly stated for others to understand and help strengthen the claim that only dural cells are labelled in explant experiments.**

We thank the reviewer for this helpful comment. Based on the reviewer's suggestion, we re-optimized dye labeling using Vybrant™ DiI Cell-Labeling Solution (Thermo Fisher, V22885), a cell membrane dye. We found that DiI effectively labeled the dura, allowing us to visualize dural cell migration into the coronal suture in a suture transplantation model (**Fig. 1h-k**). More importantly, we have also added experiments using WT suture mesenchyme and transplanted into *Gli1creER;tdT* recipient. Consistent with the dye labeling, we also observed migration of tdT+ dura cells into suture mesenchyme (**Fig. 2a-b**).

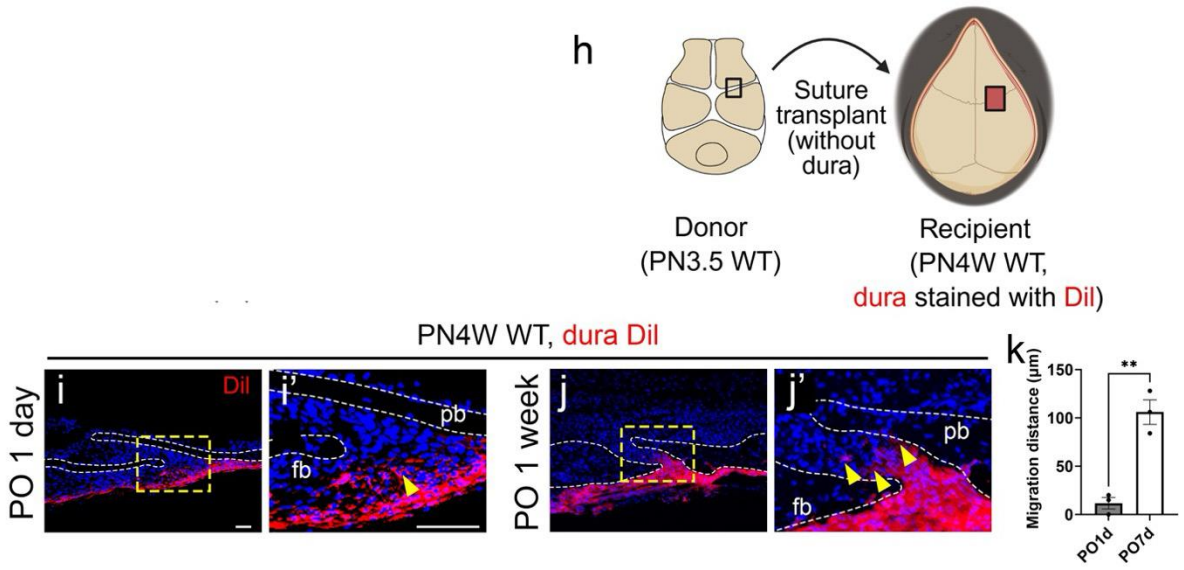


**Fig. 1: Dural cell migration to coronal suture mesenchyme during postnatal development.**

(h-k) Suture transplant model showing dural cells actively migrating into coronal suture mesenchyme. (h) Schematic drawing of suture transplantation surgery. (i) Fluorescence images showing dural cells labeled with DiI (yellow arrowheads) 1 day after suture transplantation surgery. (i') shows the enlarged image from the yellow frame in (i). (j) Fluorescence images showing DiI+ signals (yellow arrowheads) in both the dura mater and suture mesenchyme 7 days after surgery. (j') shows the enlarged image from the yellow frame in (j). (k) Quantitative data in (i', j') are presented as mean ± SEM, $p = 0.0026$, **, calculated by two-tailed unpaired t-test, Scale bar: 50 μm.

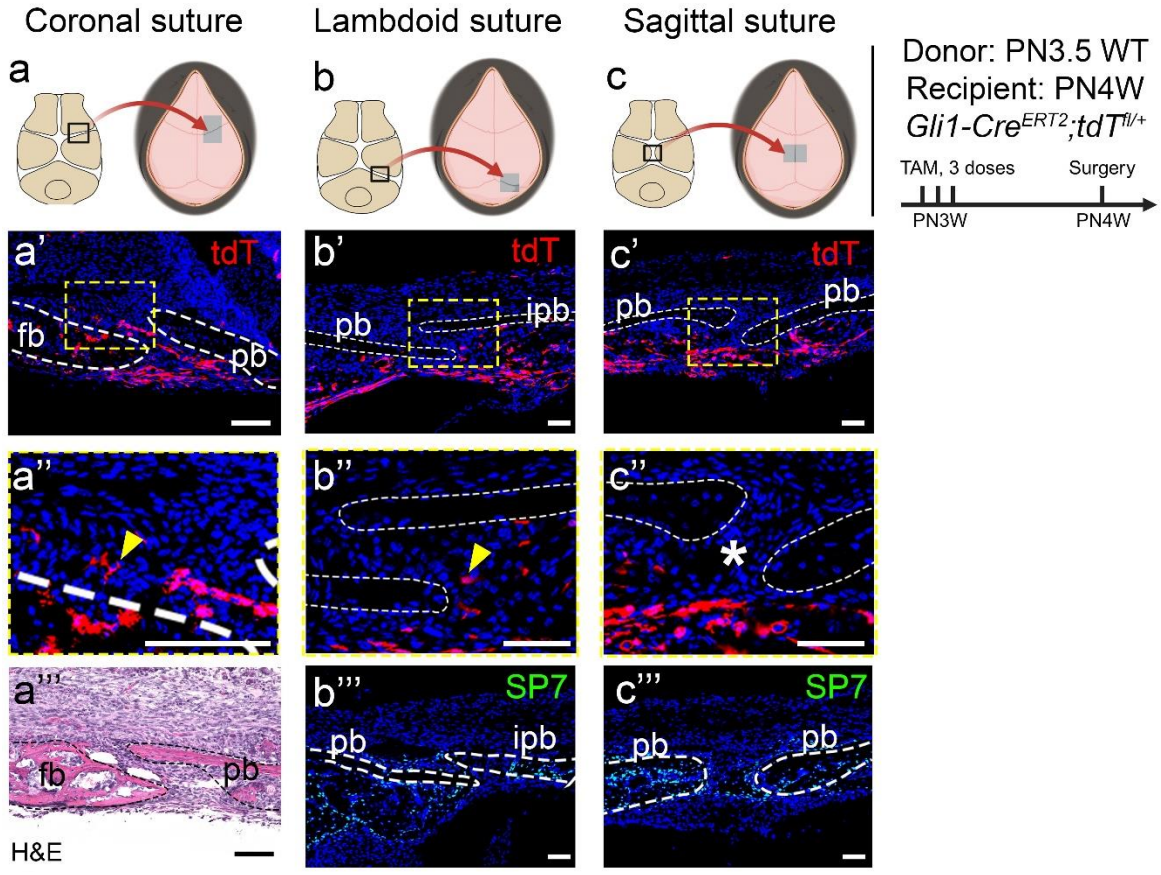


**Fig. 2: Dural cell migration is predominantly a coronal suture-specific phenomenon**

(a-c) Schematic drawings showing the surgical procedure for suture transplantation in each group for a'-c'''. (a'-c') Representative fluorescence imagesshowing dural cell migration following suture transplantation. Coronal (a), lambdoid (b), and sagittal (c) suture transplantation seven days after surgery. Donor suture boundaries are outlined by dashed lines. tdT+ dural cells from *Gli1-Cre$^{ERT2}$;tdT$^{fl/+}$* mice are shown in red, and nuclei are counterstained with DAPI in blue. Yellow

dashed boxes indicate regions shown at higher magnification in a''-c''. Scale bars: 50μm. (a''-c'') Enlarged views of a'-c'. Arrowheads indicate tdT+ cells and the asterisk denotes absence of tdT+ cells. Scale bars: 50μm. (a''') H&E staining shows the structure of the donor suture after transplantation surgery. (b'''-c''') SP7 immunostaining images showing the bone surface of the donor suture structure. Scale bars: 50μm. Fb: frontal bone, pb: parietal bone, ipb: interparietal bone.

**3. (i) Line 135: 'DuSC migratory capacity and EdU incorporation (Supplementary Fig. 2b-g), indicating enhanced migration and proliferation compared to controls…SuSCs can enhance DuSC migration and proliferation.'- While a common assumption in scratch assays, the inference of cell migration is not strictly correct without additional experiments. The increase in proliferation found when incubating DuSCs or SuSCs in suture conditioned media could be sufficient to explain the wound healing assays without requiring migration (see Ranft et al. 2010: Mechanically driven interface propagation in biological tissues, and Cochet-Escartin and Ranft et al. 2014: Border Forces and Friction Control Epithelial Closure Dynamics, or indeed ref 20 Dahmann et al. 2011). The increase in proliferation is nonetheless good evidence of stem cell behavior where division is an important part of stem cell mobilization in repair. To be confident that cell migration is increased in these assays, cell tracking, a measure of cell mixing, or cell density vs scratch closure could be assayed. As much of the field fails to recognize these limitations of scratch assays and authors continue to uphold them as tests of migration, it is not essential to change these statements in the manuscript. However, without toning down or specifying the limitations of these assays, the quality of the work is undermined and, in this case, may impact the long-Gevity of the work.**

We thank the reviewer for this thoughtful and insightful comment regarding the interpretation of scratch assays. We agree that wound closure/scratch assays reflect a combination of cell proliferation and migration, and that increased proliferation by itself could contribute to accelerated closure without necessarily requiring enhanced migration, as discussed in the cited studies[2, 3, 4].

We also observed increased EdU incorporation under these conditions, which also provides strong evidence of enhanced proliferative activity. In light of this, we have revised the text to tone down the interpretation of these assays by replacing references to "migration" with "cell mobilization"

or “wound closure,” and have added a brief statement in the Results explicitly acknowledging the limitations of scratch assays in distinguishing migration from proliferation.

Finally, to clarify whether the cell migration itself was indeed affected, we performed transwell migration assays to directly assess dural cell motility. We found that dural mesenchyme cells (DuSC) exposed to suture mesenchymal stromal cell-conditioned medium (SuSC-CM) showed increased migration, whereas inhibition of *Tgfbr2* reduced this migration response (**Supplementary Fig. 2h-k, Supplementary Fig. 5h-j**). In addition, SuSC-CM derived from *Twist1*$^{+/-}$ samples showed a diminished migration-promoting effect, and recombinant decorin treatment further reduced DuSC migration (**Fig. 6p, s, x**).

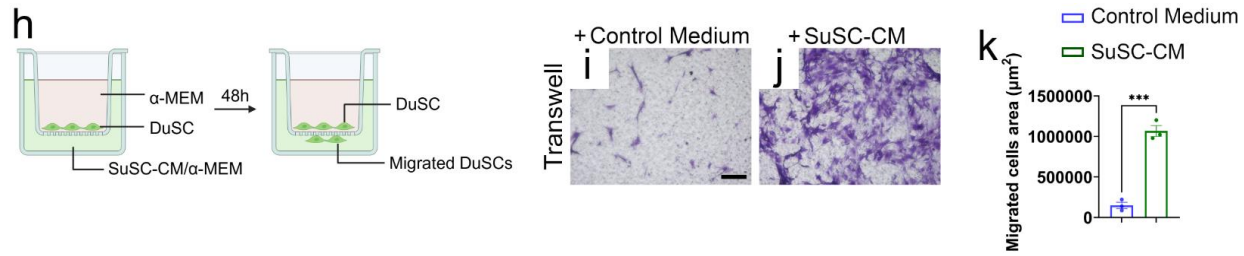


**Supplementary Fig. 2: Suture mesenchymal stromal cells promote dural cell proliferation and migration.**

(h) Diagram showing procedures of the transwell assay in (i-j). (i-j) Representative images of transwell assays showing enhanced migration ability when treated with SuSC-CM (j) compared to control medium (i). Scale bar: 200 μm. (k) Quantitative data in (i & j) are presented as mean ± SEM, $p$ = 0.0003, ***, calculated by two-tailed unpaired t-test, N = 3.

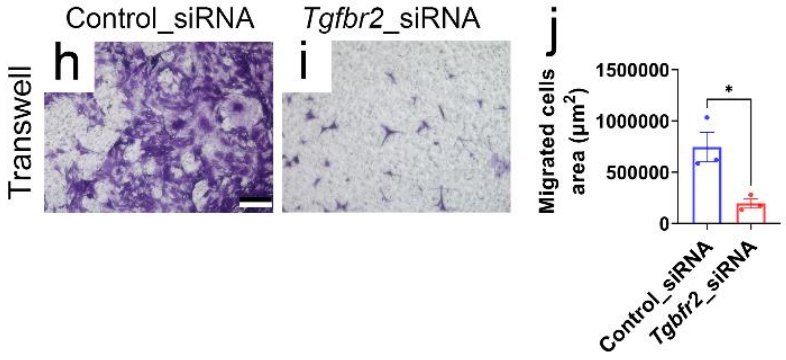

**Supplementary Fig. 5: Suture mesenchymal stromal cells promote dural cell proliferation and migration through TGFβ signaling pathway.**

(h-i) Representative images of transwell assays showing reduced migration ability following *Tgfbr2*_siRNA treatment (i) compared to control_siRNA treatment (h). Scale bar: 200 µm. (j) Quantitative data in (h & i) are presented as mean ± SEM, $p = 0.0217$, *, N = 3, calculated by two-tailed unpaired t-test.

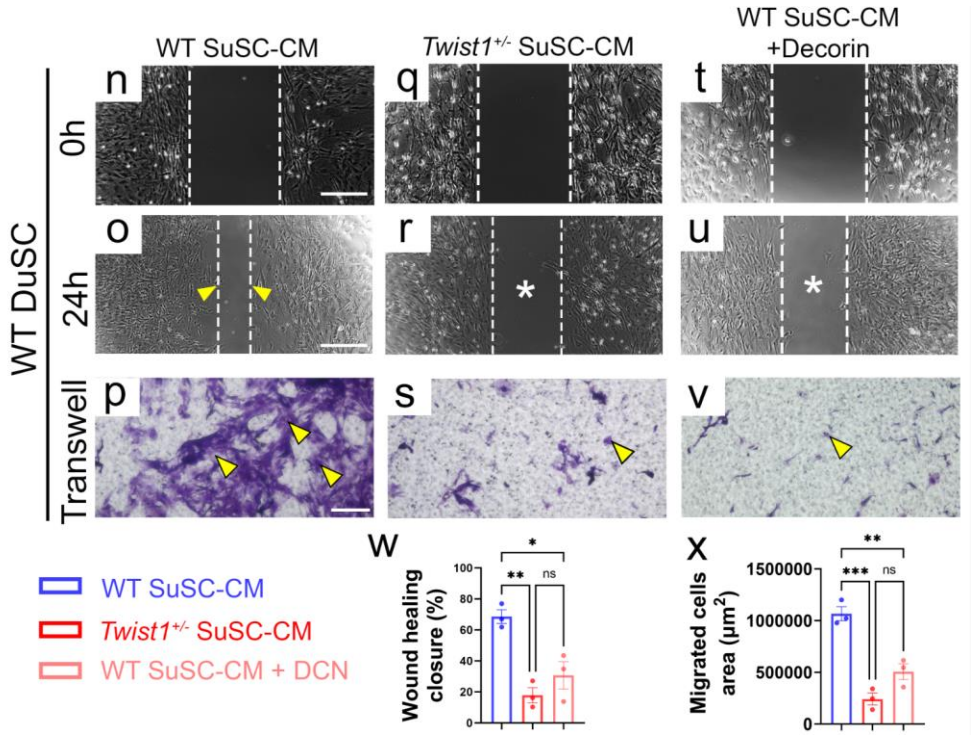


**Fig. 6: *Twist1*$^{+/-}$ mice show impaired TGFβ signaling and reduced dural cell migration.**

(n-v) Representative images of wound healing assays (n-o, q-r, t-u) and transwell assay (p, s, v) showing impaired migration ability after treatment with *Twist1*$^{+/-}$ CM (q-s) or decorin (t-v) compared to the control (n-p, yellow arrowheads). Scale bar: 200 µm. (w) Quantification of wound healing closure area in the indicated groups. Data are mean±SEM. One way ANOVA with multiple comparisons, N = 3, $p = 0.0032$, ** (WT vs. *Twist1*$^{+/-}$), $p = 0.0133$, * (WT vs. DCN), $p = 0.3902$, ns (*Twist1*$^{+/-}$ vs. DCN). (x) Quantification of migrated cell area in the indicated transwell groups. Data are mean±SEM. One way ANOVA with multiple comparisons, N = 3, $p = 0.0003$, *** (WT vs. *Twist1*$^{+/-}$), $p = 0.0027$, ** (WT vs. DCN), $p = 0.0753$, ns (*Twist1*$^{+/-}$ vs. DCN).

**3. (ii) A similar problem arises in Results for Figure 6, Line 281: 'This treatment suppressed the migration-promoting effect of SuSC-CM (Fig. 6r-s), indicating that Decorin inhibits dural cell migration.'. In the absence of cell tracking, it is not technically true that these data demonstrate Dcn as a regulator of dural cell migration. As there is no metric of cell proliferation for these samples, it is also not clear whether Dcn treatment phenocopies the Tgfβ deletion. Comparing cell density between start and end of scratch assay could be sufficient to extract an effective proliferation metric. The claim that Dcn inhibits migration would therefore be more convincing If proliferation is not increased or density is far lower despite increased proliferation.**

We thank the reviewer for this insightful comment regarding the interpretation of the scratch assay in Fig. 6. We agree that, in the absence of direct cell tracking, wound closure assays cannot definitively distinguish altered cell migration from changes in cell proliferation.

To address whether decorin affects dural cell proliferation, we performed EdU incorporation assays in DuSCs treated with SuSC-conditioned medium in the presence or absence of recombinant decorin. These analyses revealed that decorin significantly reduced EdU incorporation in DuSCs, indicating suppressed proliferative activity (**Supplementary Fig. 8a-c**).

Given these results, we have revised the text (**lines 317-322**) to avoid overinterpretation of the scratch assay data. Specifically, we now describe decorin as attenuating SuSC-CM-induced dural cell mobilization, which reflects combined effects on proliferative activity and cell motility, and we explicitly acknowledge the limitations of scratch assays in distinguishing migration from proliferation.

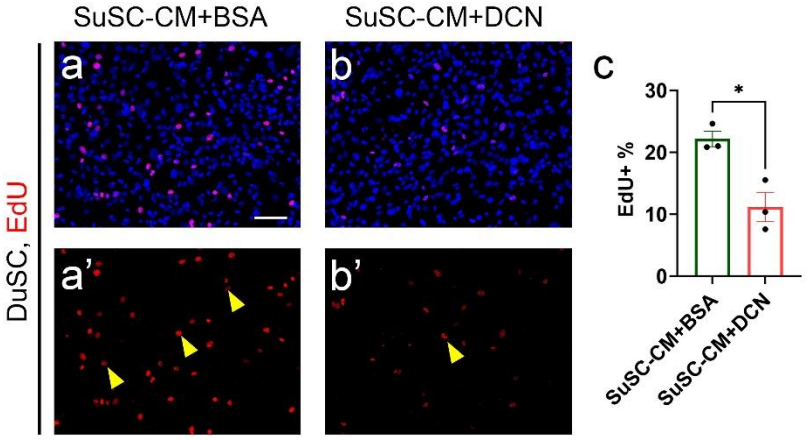

**Supplementary Fig. 8: The function of Decorin in coronal dural cells, lambdoid suture, and sagittal suture.**

(a-c) Representative EdU incorporation assays of DuSCs cultured with SuSC-conditioned medium supplemented with BSA (control; a, a') or recombinant decorin (DCN; b, b'). Upper panels (a, b) show merged images of EdU (red) and DAPI (blue), while lower panels (a', b') show EdU signal alone. Treatment with decorin markedly reduced the number of EdU+ DuSCs compared to BSA control, indicating suppressed proliferative activity in response to SuSC-derived signals. Scale bar, 100 μm. (c) Quantification data in (a-b) are presented as mean ± SEM, calculated by two-tailed unpaired t-test, $p = 0.0141$, *, N = 3.

**4. Sup fig. 2: Quantification of EdU experiments should accompany the image panels, in particular, because the cell densities appear quite different between each condition.**

We thank the reviewer for this suggestion. We have now included quantitative analyses of EdU incorporation across 3 biological replicates in **Supplementary Figs. 2, 5, and 8**.

**5. Sup Fig. 5: Although consistent with data throughout the paper, Sup Fig 5 does not demonstrate a reduced progenitor pool in animals with Tgfbr2 mutant Gli1 cells, although it does show their proliferation is reduced. Testing this claim definitively would require a metric of suture mesenchyme cell density/width or quantifying Maff, Lepr, or ccl7 expressing cells in situ or through sequencing. Toning down the title of this figure would be sufficient to address this concern.**

We thank the reviewer for this insightful comment. We have revised the title and corresponding text of revised **Supplementary Fig. 6** to more accurately reflect the data presented, focusing on reduced proliferation rather than a definitive loss of the progenitor pool. The manuscript text has been adjusted accordingly (Lines 244-247).

Additionally, we examined the expression levels of *Maff*, *Lepr*, and *Ccl7* and found that all three markers showed a marked reduction in the suture mesenchyme of *Tgfbr2* mutant mice, suggesting

a reduced progenitor cell pool in *Tgfbr2* mutants. Notably, at this point, *Gli1* levels were not yet reduced, suggesting a differential response among progenitor markers (Response letter Fig. 5).

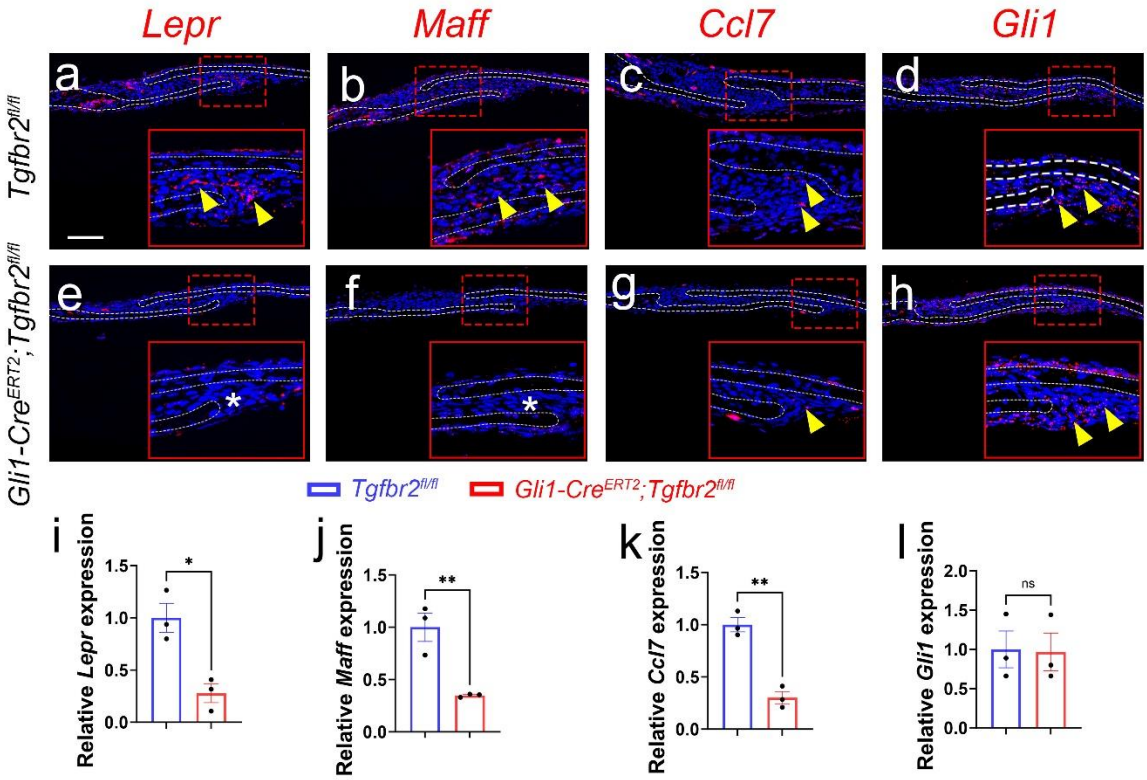


**Response letter Fig. 5: Reduced expression of suture progenitor markers in *Gli1-Cre$^{ERT2}$;Tgfbr2$^{fl/fl}$* coronal sutures.**

(a-l) RNAscope staining of *Lepr*, *Maff*, *Ccl7*, and *Gli1* (red) in PN5.5 (2 days post tamoxifen induction) control (*Tgfbr2$^{fl/fl}$*, a-d) and *Gli1-Cre$^{ERT2}$;Tgfbr2$^{fl/fl}$* mutant (e-h) coronal sutures. Boxed regions are shown at higher magnification below each panel. Yellow arrowheads indicate marker-positive cells within the suture mesenchyme. Asterisks mark regions with reduced cellularity in mutant sutures. Nuclei are stained with DAPI (blue). Dashed lines outline the suture mesenchyme. Scale bar: 100 μm.

**6. Is it known whether any mesodermal mesenchyme expresses Wnt1 postnatally? Is it possible that these cells are coming from later Wnt1 expressing cells that are not neural crest? Not essential to address but may be a concern for some and can potentially be extracted from scRNA sequencing data or other published work.**

We thank the reviewer for raising this important point. To address the possibility that postnatal mesodermal mesenchyme might express Wnt1, we examined *Wnt1* expression in the PN10 coronal suture using both RNAscope *in situ* hybridization and scRNA-seq analysis. RNAscope *in situ* staining showed almost no *Wnt1* expression in the P10 coronal suture (Response letter Fig. 6). Consistent with this, *Wnt1* expression was undetectable in suture mesenchymal cell populations in a P10 coronal suture scRNA-seq dataset. Together, these data indicate that postnatal mesodermal mesenchyme does not exhibit appreciable *Wnt1* expression, supporting the interpretation that *Wnt1*-labeled cells observed in our lineage tracing experiments are of neural crest origin rather than arising from later *Wnt1*-expressing non-neural crest cells.

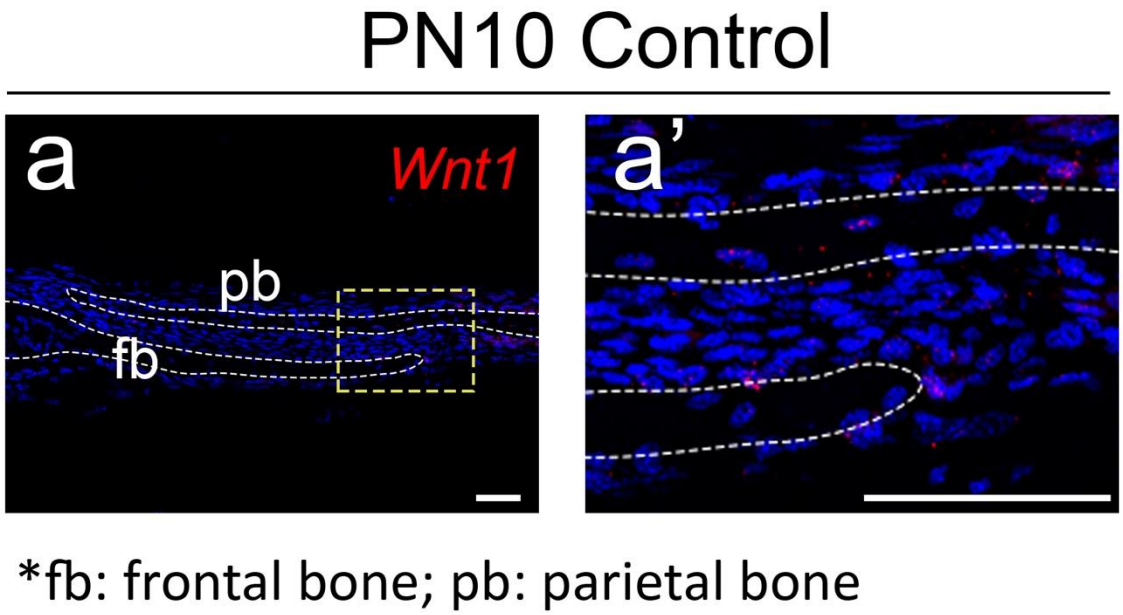


**Response letter Fig. 6: *Wnt1* expression was almost undetectable in the PN10 coronal suture.**

(a) RNAscope detection of *Wnt1* transcripts (red) in the PN10 control coronal suture. Boxed region is shown at higher magnification on the right. Nuclei are stained with DAPI (blue). Dashed lines outline the suture mesenchyme. fb, frontal bone; pb, parietal bone. Scale bar: 100 μm.

**7. Sections of mice treated with Decorin presented in Figure 7e-f appear as though bone fusion is most pronounced on the dural side of the suture. Is this consistent across samples? If so, mentioning this in the results or discussion could further bolster the claim that DuSCs replenish the suture stem cell niche as the dural aspect of the suture would be most affected**

**if the Author's hypothesis is correct. One way to express this would be to measure the width of the suture at the tips of FB and PB and through the centre of the suture. It is not necessary to add these data but these would further support the authors claims.**

We thank the reviewer for this observation. After examining multiple decorin-treated samples, we did not observe a consistent preference for dural-side suture fusion across replicates. Therefore, we did not emphasize dural-side-specific fusion in the Results or Discussion to avoid overinterpretation.


1. Jarvinen, T.A., Prince, S. Decorin: A Growth Factor Antagonist for Tumor Growth Inhibition. *Biomed Res Int* **2015,** 654765 (2015).

2. Ranft, J., Aliee, M., Prost, J., Jülicher, F., Joanny, J.-F. Mechanically driven interface propagation in biological tissues. *New Journal of Physics* **16,** (2014).

3. Dahmann, C., Oates, A.C., Brand, M. Boundary formation and maintenance in tissue development. *Nat Rev Genet* **12,** 43–55 (2011).

4. Cochet-Escartin, O., Ranft, J., Silberzan, P., Marcq, P. Border forces and friction control epithelial closure dynamics. *Biophys J* **106,** 65–73 (2014).

**REVIEWERS' COMMENTS**

**Reviewer #1 (Remarks to the Author):**

**The authors have addressed my queries in depth through additional experiments. Specifically, the expansion of the allograft suture transplantation experiments, as detailed in the revised Figure 2, has significantly strengthened the rigor of the current findings.**

**1. Regarding my previous second point, the authors provided evidence that Tgfrb2 is selectively expressed in the dura below the coronal suture (Fig.3h), unlike in other sutures where Tgfrb2 expression is more widespread (Supplementary Fig. 7j,l,n). The description of these results in the revised main text (Lines 254-265) should be improved. To better contextualize these findings, the authors should emphasize that Tgfrb2 is most prominently expressed in the dura of the coronal suture, but not in that of other sutures. This claim can also be supported quantitatively by quantifying the ISH signal in the dura across four different sutures.**

We thank the reviewer for this helpful suggestion. We have revised the description in the main text (Lines 271-286) to better emphasize that *Tgfbr2* is most prominently expressed in the dura underlying the coronal suture. We have also performed quantitative analysis as advised by the reviewer. Our conclusion regarding the distribution of *Tgfbr2* expression in the dura across four different sutures is supported by consistent qualitative differences observed across multiple sections (Supplementary Fig. 10o)

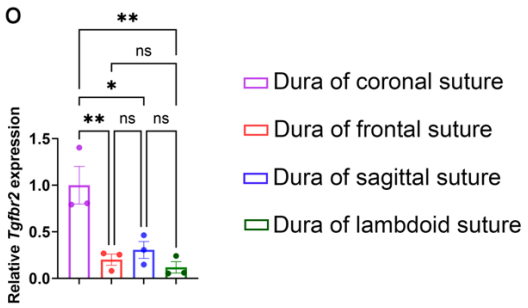


*fb: frontal bone; pb: parietal bone, ipb: interparietal bone

**Supplementary Fig. 10: Loss of *Tgfbr2* in Gli1+ progenitor cells does not lead to frontal, sagittal, or lambdoid suture fusion.**

(o) Quantitative data in (j, l, n) are presented as mean ± SEM, calculated by one-way ANOVA with multiple comparisons, showing higher expression in coronal versus frontal ($p$ = 0.0061), sagittal ($p$ = 0.0137), and lambdoid sutures ($p$ = 0.0034), with no differences among frontal, sagittal, and lambdoid groups ($p$ = 0.9216, 0.9580, and 0.6892).

**2. The switch from Q-tracker organ culture to DiI transplantation is reasonable, enhancing the rigor of the study. However, to demonstrate the validity of this approach, the authors would need an additional control to definitively show that the dura DiI signal expansion into the suture mesenchyme after transplantation is not due to passive diffusion. A critical control would be sagittal suture transplantation onto a DiI-labelled dura (of the sagittal suture), which should not show any dura DiI signal in the suture mesenchyme after transplantation, if the authors' premise is correct.**

We thank the reviewer for this important suggestion regarding the need to exclude the possibility of passive diffusion of the DiI signal. We would like to clarify that such a control is already present in our current data. Specifically, in Figures 6a-e, we performed transplantation experiments using *Twist1*$^{+/-}$ dura, in which we did not observe significant DiI signals within the *Twist1*$^{+/-}$ suture mesenchyme. This result demonstrates that the DiI signal does not passively diffuse into the suture, but instead depends on the intrinsic migratory capacity of dural cells. We have clarified this point

in the revised manuscript (Lines 313-315) to assist in the interpretation of these findings.

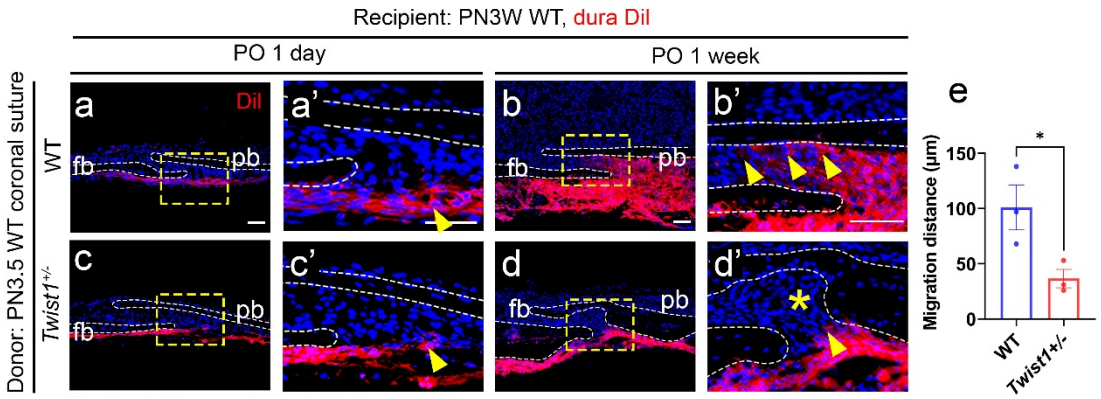


**Fig. 6: *Twist1*$^{+/-}$ mice show impaired TGFβ signaling and reduced dural cell migration.**

(a-d) Fluorescence images of DiI+ signals (red) in WT and *Twist1*$^{+/-}$ coronal suture transplanted into coronal area at 1 and 7 days post-suture transplantation. (a'-d') Magnified views of the boxed regions in (a-d). Arrowheads and asterisks indicate presence or absence of DiI signals, respectively. (e) Quantification of (b', d') (mean ± SEM, p = 0.0427, *, N = 3, two-tailed unpaired t-test).

**3. Some of the important information added in response to the reviewer's comments is exclusively available as reviewer-only figures, with no description or data added to the main text. The findings regarding other potential signals mediating dure-to-suture interactions (Response letter Fig.1), demonstration of suture transplantation surgery procedure (Response letter Fig.2), co-localization of TGFb ligands and decorin in coronal sutures (Response letter Fig.3), and the specificity of tdT to the dura (Rbp1) are all essential for interpreting the results of the current manuscript. They should be included in Supplementary Figures and mentioned in the main text.**

We thank the reviewer for this important suggestion. In response, we have now incorporated these previously reviewer-only figures into the Supplementary Information. Specifically, the findings regarding additional candidate signals mediating dura-to-suture interactions (former Response letter Fig. 1), the demonstration of the

suture transplantation procedure (former Response letter Fig. 2), the co-localization of TGFβ ligands and decorin in coronal sutures (former Response letter Fig. 3), and the specificity of tdTomato labeling to the dura (Rbp1, former Response letter Fig. 4) have all been included as revised Supplementary Figures 9, 2, 12, and 5, respectively. These data are now incorporated into the revised main text (Lines 100, 173-175, 248-263, 357-361) as suggested by the reviewer.

**Reviewer #2 (Remarks to the Author):**

**Chen et al. present an impressive revision of their previous submission which suggested dural cell migration mediated by Tgfbeta pathway activity is uniquely required for coronal suture patency. Their previous ex vivo culture experiments have been replaced by far more convincing in vivo grafting experiments that recapitulate previous findings and add significantly to the narrative. Taken together, the additional experiments strongly support the author's assertion that disrupted Tgfbeta activity, modulated by extracellular decorin, contributes to the pathophysiology of Saethre-Chotzen syndrome and explains differences in suture fusion across the skull cap.**

**The author's heroic efforts to confirm their hypothesis in vivo are important additions to this manuscript. These are convincing experiments with broad implications for disease and skull development generally. The references to cell mobilisation are well constructed and satisfy intellectual concerns in the prior drafts while also enriching the conclusions of the work. Overall, this reviewer is satisfied with the changes to the submitted work and am excited by the findings!**

We thank the reviewer for the positive evaluation of our revised manuscript and for the encouraging comments. We are grateful for the reviewer's valuable suggestions, which have significantly strengthened our study.

Sincerely.

Yang Chai. DDS, PhD
University Professor
Center for Craniofacial Molecular Biology
University of Southern California
ychai@usc.edu